Study of SUSY signatures at the Fermilab Tevatron in models with near mass degeneracy of the lightest chargino and neutralino

John F. Gunion and Stephen Mrenna
Davis Institute for High Energy Physics, University of California, Davis, California 95616
(Received 8 June 1999; revised manuscript received 1 October 1999; published 24 May 2000)

For some choices of soft supersymmetry (SUSY)-breaking parameters, the lightest supersymmetric particle (LSP) is a stable neutralino $\tilde{\chi}_1^0$, the NLSP is a chargino $\tilde{\chi}_1^\pm$ almost degenerate in mass with the LSP ($\Delta m_{\tilde{\chi}_1} \equiv m_{\tilde{\chi}_1^\pm} - m_{\tilde{\chi}_1^0} \sim m_\pi -$ few GeV), and all other sparticles are relatively heavy. In this case, detection of sparticles in the usual, supergravity (MSUGRA)-motivated signals will be difficult, since the decay products in $\tilde{\chi}_1^\pm \to \tilde{\chi}_1^0 \ldots$ will be very soft, and alternative signals must be considered. Here, we study the viability of signatures at the Fermilab Tevatron based on highly ionizing charged tracks, disappearing charged tracks, large impact parameters, missing transverse energy, and a jet or a photon, and determine the mass reach of such signatures assuming that only the $\tilde{\chi}_1^\pm$ and $\tilde{\chi}_1^0$ are light. We also consider the jet$+\not{E}_T$ and $\gamma+\not{E}_T$ signatures assuming that the gluino is also light with $m_{\tilde{g}} \sim m_{\tilde{\chi}_1^\pm}$. We find that the mass reach is critically dependent upon $\Delta m_{\tilde{\chi}_1}$ and $m_{\tilde{g}} - m_{\tilde{\chi}_1^\pm}$. If $\Delta m_{\tilde{\chi}_1}$ is sufficiently big that $c\tau(\tilde{\chi}_1^\pm) \lesssim$ few cm and $m_{\tilde{g}}$ is large, there is a significant possibility that the limits on $m_{\tilde{\chi}_1^\pm}$ based on CERN LEP2 data cannot be extended at the Fermilab Tevatron. If $c\tau(\tilde{\chi}_1^\pm) >$ few cm, relatively background-free signals exist that will give a clear signal of $\tilde{\chi}_1^\pm$ production (for some range of $m_{\tilde{\chi}_1^\pm}$) even if $m_{\tilde{g}}$ is very large.

PACS number(s): 12.60.Jv, 11.30.Pb, 13.85.−t, 14.80.Ly

I. INTRODUCTION

In minimal supergravity (MSUGRA) models, the soft supersymmetry-(SUSY) breaking parameters for the gauginos satisfy a common boundary condition at the ground unified theory (GUT) scale, leading to a relatively large mass splitting between the lightest chargino and the lightest neutralino [which is most often the lightest supersymmetric particle (LSP)]. This large mass splitting can lead to a large missing energy signal which facilitates the discovery of SUSY. However, for different boundary conditions, the $\tilde{\chi}_1^\pm$ and $\tilde{\chi}_1^0$ are very degenerate in mass, and discovering SUSY may be more challenging or, at least, more difficult to fully interpret. This arises naturally in two scenarios.

(1) $M_2 < M_1 \ll |\mu|$. As reviewed in Ref. [1], this hierarchy occurs when the gaugino masses are dominated by or entirely generated by loop corrections. This arises in the O-II superstring model [2–5] and the closely related models in which SUSY breaking arises entirely from the conformal anomaly [6,7], or when SUSY is broken by an F term that is a member of the **200** representation contained in $(\mathbf{24} \times \mathbf{24})_{\rm symmetric} = \mathbf{1} \oplus \mathbf{24} \oplus \mathbf{75} \oplus \mathbf{200}$ [8].

As examples of particular values for the gaugino mass parameters at the scale M_U (M_Z), the O-II model with $\delta_{\rm GS} = -4$ yields $M_3:M_2:M_1 = 1:5:10.6$ (6:10:10.6), the O-II model with $\delta_{\rm GS} = 0$ (equivalent to the simplest version of the conformal anomaly approach) yields $M_3:M_2:M_1 = 3:1:33/5$ (3:0.3:1), and the **200** model yields 1:2:10 (6:4:10). As a result:

In the **200** model and the O-II $\delta_{\rm GS} = 0$ (or pure conformal anomaly) model, M_2 is substantially below M_1 and the (tree-level) value of $\Delta m_{\tilde{\chi}_1} \equiv m_{\tilde{\chi}_1^\pm} - m_{\tilde{\chi}_1^0}$ can be very small.

In the O-II $\delta_{\rm GS} = -4$ case, M_2 is only slightly less than M_1 at low energies, but still $\Delta m_{\tilde{\chi}_1} <$ a few GeV is very typical. $\Delta m_{\tilde{\chi}_1} < 1$ GeV is possible if $|\mu| \gtrsim 1$ TeV or if $\tan\beta$ is not large and renormalization group equation (RGE) electroweak symmetry breaking is imposed [4].

In the **200** model, and especially the O-II $\delta_{\rm GS} = -4$ model, both $m_{\tilde{\chi}_2^0}$ and $m_{\tilde{g}}$ are typically quite close to the common $\tilde{\chi}_1^\pm, \tilde{\chi}_1^0$ mass, and it is natural for the squark and slepton masses to be much heavier than any of the gaugino masses. Typical values of $|\mu|$ required by RGE electroweak symmetry breaking are large, implying that the higgsino $\tilde{\chi}_2^\pm$, $\tilde{\chi}_3^0$, and $\tilde{\chi}_4^0$ states are very heavy.

In the O-II $\delta_{\rm GS} = 0$ (or conformal anomaly) model, the gluino is typically very heavy compared to the chargino.

(2) $|\mu| \ll M_{1,2}$. In this case, the $\tilde{\chi}_1^\pm$, the $\tilde{\chi}_1^0$, and the $\tilde{\chi}_2^0$ are all closely degenerate in mass and higgsino-like, while the gaugino states are much heavier. Extreme degeneracy, $\Delta m_{\tilde{\chi}_1} < 1$ GeV, is only achieved for $M_{1,2} \gtrsim 5$ TeV. The squark and slepton masses might also be large. Currently, there is less theoretical motivation for this scenario.

Thus, the exact value of $\Delta m_{\tilde{\chi}_1}$ is model dependent. However, it is generally true that $\Delta m_{\tilde{\chi}_1} < m_\pi$ is difficult to achieve. This is because the one-loop electroweak radiative corrections [9] give a positive contribution to $\Delta m_{\tilde{\chi}_1}$, that is typically $\gtrsim m_\pi$, which must be added to the tree-level value of $\Delta m_{\tilde{\chi}_1}$. In scenario (1), a useful approximation to the tree-level result when $|M_{1,2}| \ll |\mu|$ is

$$\Delta m_{\tilde{\chi}_1}(\text{tree}) \simeq \frac{m_W^4 \tan^2\theta_W}{(M_1 - M_2)\mu^2} \sin^2 2\beta. \tag{1.1}$$

From this we see that if $M_1 - M_2 > 0$, then $\Delta m_{\tilde{\chi}_1}(\text{tree}) > 0$ and $\Delta m_{\tilde{\chi}_1} > m_\pi$ is inevitable (see, e.g., the $\Delta m_{\tilde{\chi}_1}$ graphs in [4]). Even though it does not arise in the conformal anomaly or O-II model cases, there is no particular reason to exclude the possibility that $|M_2| < |M_1|$ but $M_1 - M_2 < 0$. For such cases, $\Delta m_{\tilde{\chi}_1}$ values substantially below m_π are possible.

 ©2000 The American Physical Society

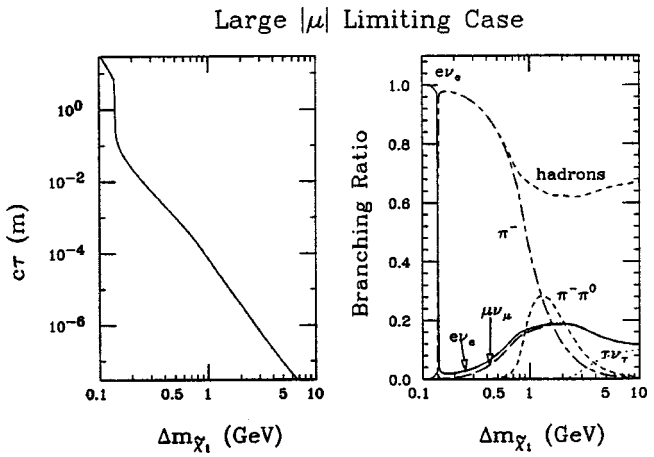

FIG. 1. The $c\tau$ and branching ratios for $\tilde{\chi}_1^-$ decay as a function of $\Delta m_{\tilde{\chi}_1} \equiv m_{\tilde{\chi}_1^\pm} - m_{\tilde{\chi}_1^0}$ for the $M_2 < M_1 \ll |\mu|$ scenario. From Ref. [5].

Thus, we will explore the phenomenology as a function of $\Delta m_{\tilde{\chi}_1}$ even for $\Delta m_{\tilde{\chi}_1} < m_\pi$. Nonetheless, it should be understood that currently popular models predict $\Delta m_{\tilde{\chi}_1}$ values in the range from slightly above m_π to several GeV. As we shall see, this is the range for which supersymmetry signals are very difficult to detect. And, as already stated, in scenario (2), the tree-level value of $\Delta m_{\tilde{\chi}_1}$ is normally substantially larger than m_π, and the one-loop corrections do not have much influence on the phenomenology. Supersymmetry detection is almost certain to be difficult in this case.

The neutralino and chargino couplings to W and Z bosons (in the absence of CP violation) depend on M_1, M_2, μ, and $\tan\beta$. For the cases considered above, the production rates for the lighter $\tilde{\chi}_1^\pm$, $\tilde{\chi}_1^0$, and $\tilde{\chi}_2^0$ states have the following pattern:

(1) When $M_2 < M_1 \ll |\mu|$, the $Z \to \tilde{\chi}_1^0 \tilde{\chi}_1^0$, $Z \to \tilde{\chi}_1^0 \tilde{\chi}_2^0$, $Z \to \tilde{\chi}_2^0 \tilde{\chi}_2^0$, and $W^\pm \to \tilde{\chi}_1^\pm \tilde{\chi}_2^0$ cross sections are all small, while Z, $\gamma \to \tilde{\chi}_1^+ \tilde{\chi}_1^-$ and $W^\pm \to \tilde{\chi}_1^\pm \tilde{\chi}_1^0$ can have large rates.

(2) When $|\mu| \ll M_{1,2}$, the Z, $\gamma \to \tilde{\chi}_1^+ \tilde{\chi}_1^-$, $Z \to \tilde{\chi}_1^0 \tilde{\chi}_2^0$, $W^\pm \to \tilde{\chi}_1^\pm \tilde{\chi}_1^0$, and $W^\pm \to \tilde{\chi}_1^\pm \tilde{\chi}_2^0$ rates will be large [but smaller than the unsuppressed channel rates in scenario (1)] and $Z \to \tilde{\chi}_1^0 \tilde{\chi}_1^0$, $Z \to \tilde{\chi}_2^0 \tilde{\chi}_2^0$ are suppressed.

Therefore, some of the sparticle production rates can be substantial, but this does not guarantee detection.

The most critical ingredients in the phenomenology of the class of models being considered are the lifetime (or decay distance $c\tau$) and the decay modes of the $\tilde{\chi}_1^\pm$, which in turn depend almost entirely on $\Delta m_{\tilde{\chi}_1}$ when the latter is small. The $c\tau$ and branching ratios of the $\tilde{\chi}_1^\pm$ as a function of $\Delta m_{\tilde{\chi}_1}$ have been computed in Ref. [5] (see also the closely related computation for a nearly degenerate heavy lepton pair $(L^\pm, L^0)$ in Ref. [10]) and are illustrated in Fig. 1 for scenario (1). For $\Delta m_{\tilde{\chi}_1} < m_\pi$, only $\tilde{\chi}_1^\pm \to e^\pm \nu_e \tilde{\chi}_1^0$ is important and $c\tau > 10\,\mathrm{m}$. Once $\Delta m_{\tilde{\chi}_1} > m_\pi$, the $\tilde{\chi}_1^\pm \to \pi^\pm \tilde{\chi}_1^0$ mode turns on and is dominant for $\Delta m_{\tilde{\chi}_1} \lesssim 800\,\mathrm{MeV}$, at which point the multipion modes start to become important: correspondingly, one finds $c\tau \lesssim 10-20\,\mathrm{cm}$ for $\Delta m_{\tilde{\chi}_1}$ just above m_π decreasing to $c\tau \sim 100\,\mu\mathrm{m}$ by $\Delta m_{\tilde{\chi}_2} \sim 1\,\mathrm{GeV}$.

For later reference, we present in Table I the specific $c\tau$ values as a function of $\Delta m_{\tilde{\chi}_1}$ that we have employed in our Monte Carlo studies.

Since experimental details are particularly important for our analysis, we briefly review some of the components of a canonical Run II detector (e.g., CDF or DØ) ordered according to increasing radial distance from the beam.

An inner silicon vertex (SVX) detector extending radially from the beam axis. The Collider Detector at Fermilab (CDF) run II vertex detector has layers at $r \sim 1.6$, 3, 4.5, 7, 8.5, and 11 cm (the first and second layers are denoted $L00$ and $L0$, respectively) extending out to $z = \pm 45\,\mathrm{cm}$ [11]. The DØ SVX has four layers (but two are double sided), with the first at 2.5 cm and the last at 11 cm.

A central tracker (CT) extending from 15 to 73 cm (DØ) or from roughly 20 to 130 cm (CDF).

A thin preshower layer (PS).

An electromagnetic calorimeter (EC) and hadronic calorimeter (HC).

The inner-most muon chambers (MC), starting just beyond the HC. The DØ inner central muon chambers form (very roughly) a box, the ends of which (through which the beam passes) are a $5.4\,\mathrm{m} \times 5.4\,\mathrm{m}$ square and the sides of which are 8 in. in length. The sides (parallel to the beams) cover $|\eta| < 1$, while the ends are instrumented out to $|\eta| < 2$. The CDF inner muon chambers form roughly a barrel at a radial distance of 3.5 m with length of about 5 m. There is no muon detection capability on the ends of the barrel, so only $|\eta| < 0.6$ is covered by the inner chambers.

Both CDF and DØ will have a precise time-of-flight measurement (TOF) for any charged particle that makes it to the muon chambers.

One fact that is important for our analysis is that the SVX, CT, and PS can all give (independent) measurements of the ionization energy loss (dE/dx) of a charged track passing through them. This information can be used to distinguish a heavily ionizing chargino [which would be $\geqslant$ twice minimal ionizing (2MIP) for $\beta\gamma \leqslant 0.85$] from an isolated minimally ionizing particle (1MIP). For example, at DØ the rejection against isolated 1MIP tracks will be few$\times 10^{-3}$, few $\times 10^{-3}$, and $\sim 10^{-1}$ for tracks that pass through the SVX,

TABLE I. Summary of $c\tau$ values as a function of $\Delta m_{\tilde{\chi}_1^-}$ as employed in Monte Carlo simulations.

$\Delta m_{\tilde{\chi}1}$(MeV)	125	130	135	138	140	142.5	150
$c\tau$(cm)	1155	918.4	754.1	671.5	317.2	23.97	10.89
$\Delta m_{\tilde{\chi}1}$(MeV)	160	180	185	200	250	300	500
$c\tau$(cm)	6.865	3.719	3.291	2.381	1.042	0.5561	0.1023

TABLE II. Summary of detector components referred to in the text.

Component	Description
SVX	Silicon vertex detector from close to beam pipe to ~11 cm.
CT	Central tracker starting just past SVX.
PS	Preshower just outside the tracker.
EC	Electromagnetic calorimeter.
HC	Hadronic calorimeter.
TOF	Time-of-flight measurement after HC and just before MC.
MC	Muon chamber with first layer after the HC and just beyond the TOF.

CT, and PS respectively, with an efficiency of 90% for tracks with[1] $\beta\gamma<0.85$ [12]. At CDF, the discrimination factors should be roughly similar [13]. Because of correlations, one cannot simply multiply these numbers together to get the combined discrimination power of the SVX, CT, and PS for an isolated track that passes through all three; for such a track with $\beta\gamma<0.85$, the net discrimination factor would probably be of order few$\times 10^{-5}$. A summary of our shorthand notations for detector components appears in Table II.

In the following, we consider several possible signals, many of which are unique to SUSY scenarios with near mass degeneracies: (a) LHIT and TOI, (b) DIT, (c) STUB and KINK, (d) HIP+KINK, (e) HIP, (f) $\gamma+\not{E}_T$ and jets$+\not{E}_T$, and (g) standard MSUGRA signals. Abbreviated definitions of these signals are presented in Table III. They will be elaborated upon later.

In this analysis, we make numerical estimates of the background and signal rates after cuts for these various signals. For measurements at the Tevatron in Run II, we have made several assumptions, including triggering capabilities and fake rejection rates. For example, in the time of flight (TOF) analysis, the possible cosmic-ray background is not included. Only once the Tevatron starts running will the experiments really know what the fake rates are and which triggering choices are acceptable. Some of the numbers used are based on educated guesses, backed up by discussions with CDF and DØ experimentalists. The numbers used are correct to the best of our knowledge, and our sources (people) are listed in the acknowledgements. One aim of this study is to expose the issues that experimentalists will need to consider.

II. COLLIDER PHENOMENOLOGY OF DEGENERATE MODELS

Although our main focus will be on Tevatron in Run II, we first review the constraints on degenerate scenarios from searches for $\tilde{\chi}_1^+\tilde{\chi}_1^-$ production at LEP and LEP2.

[1]It is a combination of Landau fluctuations, electronic noise and, most importantly in hadron collisions, overlapping soft tracks that is responsible for these discrimination factors being worse than one might naively expect.

A. Lepton colliders

As discussed above and in Refs. [3–5], collider phenomenology depends crucially on $\Delta m_{\tilde{\chi}_1}$. Most importantly, SUSY detection depends on which aspects (if any) of the $\tilde{\chi}_1^+\tilde{\chi}_1^-$ final state are visible.

If the $\tilde{\chi}_1^\pm$ decay products are soft and the $\tilde{\chi}_1^+\tilde{\chi}_1^-$ production is otherwise untagged, the event may be indistinguishable from the large $e^+e^-\to e^+e^-\gamma\gamma\to e^+e^-+$soft background. In this case, one will need to tag $\tilde{\chi}_1^+\tilde{\chi}_1^-$ production, for example, from the initial- or final-state radiation of a photon, denoted as ISR [3]. Even with an ISR tag, it is possible that the $\tilde{\chi}_1^+$ and $\tilde{\chi}_1^-$ will both be effectively invisible because of the softness of their decay products and the lack of a vertex detector signal. In this case, $\gamma\tilde{\chi}_1^+\tilde{\chi}_1^-$ production is observable as a $\gamma\not{M}$ signature, which is distinguishable from the $\gamma\nu\bar{\nu}$ process by the threshold in the missing mass variable $\not{M}=\sqrt{(p_{e^-}+p_{e^+}-p_\gamma)^2}$ at $\not{M}=2m_{\tilde{\chi}_1^\pm}$. The exact mass reach in $m_{\tilde{\chi}_1^\pm}$ depends upon available luminosity and machine energy. Estimates were presented in Ref. [3], which we summarize for the $M_2<M_1\ll|\mu|$ scenario (1). At the CERN e^+e^- collider LEP2, for $L=125\,\mathrm{pb}^{-1}$ per experiment, no improvement was found over the $m_{\tilde{\chi}_1^\pm}<45\,\mathrm{GeV}$ limit coming from LEP1 Z-pole data on $Z\to$invisible decay channels. At the Next Linear Collider the prospects are better: with $L=50\,\mathrm{fb}^{-1}$, the $\gamma\not{M}$ channel will be sensitive up to $m_{\tilde{\chi}_1^\pm}\sim 200\,\mathrm{GeV}$. In scenario (2), both $\gamma\tilde{\chi}_1^+\tilde{\chi}_1^-$ and $\gamma\tilde{\chi}_1^0\tilde{\chi}_2^0$ will have significant rates and a common threshold in $\not{M}$, and the discovery reach is similar to that in scenario (1).

The experimental situation is greatly improved if the LHIT signal can be employed or if the soft pions from the $\tilde{\chi}_1^\pm$ decays in $\gamma\tilde{\chi}_1^+\tilde{\chi}_1^-$ events can be detected. This is clearly illustrated by the analysis from DELPHI at LEP2 [14]. This analysis employs (in order of increasing radius from the beampipe) central inner detector (ID) and time projection chamber (TPC) tracking devices and the ring-imaging Cherenkov device (RICH). (For details regarding these devices, please refer to Ref. [14].)

For scenario (1) or (2), when $\Delta m_{\tilde{\chi}_1}\lesssim 200\,\mathrm{MeV}$, the charginos are sufficiently long lived to produce one of two signals for $\tilde{\chi}_1^+\tilde{\chi}_1^-$ production.

TABLE III. Summary of signals. MIP refers to a minimally ionizing particle such as a $\beta=1$ muon. For detector component notation, see Table II.

Signal	Definition
LHIT	Long, heavily ionizing ($\geqslant$ 2MIP's as measured by SVX+CT+PS), large-p_T track that reaches the MC. The energy deposit in the HC in the track direction must be consistent with expected ionization energy deposit for the β measured (using TOF and/or SVX+CT+PS), i.e., no hadronic energy deposit.
TOF	A large-p_T track seen in the SVX and CT along with a signal in the TOF delayed by 500 ps or more (vs a particle with $\beta=1$). HC energy deposit (in the direction of the track) is required to be consistent with the ionization expected for the measured β (i.e., no hadronic deposit).
DIT	An isolated, large-p_T track in the SVX and CT that fails to reach the MC and deposits energy in the HC no larger than that consistent with ionization energy deposits for the measured (using SVX+CT+PS) β. Heavy ionization in the SVX+CT+PS, corresponding to $\beta<0.8$ or $\beta<0.6$ (DIT8 or DIT6), may be required.
KINK	A track that terminates in the CT, turning into a soft, but visible, charged-pion daughter track at a substantial angle to parent.
STUB	An isolated, large-p_T (as measured using SVX) track that registers in all SVX layers, but does not pass all the way through the CT. Energy deposits in the EC and HC in the direction of the track should be minimal.
SNT	One or more STUB tracks with no additional trigger. Heavy ionization of the STUB in the SVX, corresponding to $\beta<0.6$ (SNT6), may be required.
SMET	One or more STUB tracks with an $\not{E}_T>35$ GeV trigger. Heavy ionization of the STUB in the SVX, corresponding to $\beta<0.6$ (SMET6), may be required.
HIP	A high-impact-parameter ($b\geqslant 5\sigma_b$) track in the SVX, with large $\not{E}_T$ triggering, perhaps in association with a visible KINK in the SVX.
$\gamma+\not{E}_T$	Isolated, large-p_T photon and large $\not{E}_T$.
Monojet+$\not{E}_T$	Large-p_T jet and large $\not{E}_T$.
MSUGRA-like	jet(s)+$\not{E}_T$, trileptons, like-sign dileptons, etc., except that the cross section for the $\tilde{\chi}_1^{\pm}\tilde{\chi}_2^0$ trilepton signal can be suppressed.

(a) For $\Delta m_{\tilde{\chi}_1}\lesssim m_\pi$, the charginos produce heavily ionizing tracks (LHIT's) recognizable by high specific ionization in the TPC or by the absence of Cherenkov light in the RICH.

(b) For $m_\pi\lesssim\Delta m_{\tilde{\chi}_1}\lesssim 200$ MeV, both the charginos and their soft pion daughters yield visible tracks in the central tracking devices (the ID and the TPC, located in the region $10\,\text{cm}<r<1$ m). A clean signal is provided by demanding two primary particle tracks emitted in opposite hemispheres, each decaying to a soft, charged daughter moving at a substantial angle to the primary track. This type of signal is called a KINK.

Note that no additional trigger is required for either signal. We summarize the DELPHI results for scenario (1). By combining (a) and (b), DELPHI is able to exclude $m_{\tilde{\chi}_1^{\pm}}$ out to nearly the kinematic limit (currently 92 GeV) for any $\Delta m_{\tilde{\chi}_1}<200$ MeV if the sneutrino is heavy (implying large $\tilde{\chi}_1^+\tilde{\chi}_1^-$ production rate) or $\Delta m_{\tilde{\chi}_1}<60$ MeV if the sneutrino is light (implying suppressed production rate).

When $\Delta m_{\tilde{\chi}_1}\gtrsim 3$ GeV, the decay products of the $\tilde{\chi}_1^{\pm}$ become easily visible, and the standard MSUGRA search strategies apply. For a heavy sneutrino, the $\tilde{\chi}_1^{\pm}$ is excluded out to about 90 GeV for $\Delta m_{\tilde{\chi}_1}=3$ GeV rising to 92 GeV for

$\Delta m_{\tilde{\chi}_1} > 10\,\mathrm{GeV}$. For a light sneutrino, the $\tilde{\chi}_1^+\tilde{\chi}_1^-$ cross section is smaller and the limit only extends to ~65–75 GeV for $3\,\mathrm{GeV} < \Delta m_{\tilde{\chi}_1} < 10\,\mathrm{GeV}$.

For $200\,\mathrm{MeV} \lesssim \Delta m_{\tilde{\chi}_1} \lesssim 3\,\mathrm{GeV}$, the chargino tracks are not long enough to use the ID/TPC KINK signature, and the chargino decay products are too soft to provide a clear signature on their own. In this case, one must overcome the very large $\gamma\gamma$ collision background rate for events containing only soft tracks by tagging the chargino pair production event. As proposed in Ref. [3], DELPHI employs an initial state radiation (ISR) photon tag. The photon is required to have energy above 4 GeV and the recoil mass $\not{M}$ is required to be above 96 GeV (which eliminates all but the virtual Z tail of $\gamma Z^* \to \gamma\nu\bar{\nu}$ events and the nonresonant contributions). Visible energy (excluding the photon) is required to be less than a few percent of $\sqrt{s}$ (the exact value depends upon the $\Delta m_{\tilde{\chi}_1}$ value being probed). Finally, in order to essentially eliminate the $\gamma\nu\bar{\nu}$ background, the event is required to contain soft charged tracks consistent with the isolated pions expected from the chargino decays. DELPHI observed no events after all cuts. For a heavy sneutrino, this excludes $m_{\tilde{\chi}_1^\pm} \lesssim 70\,\mathrm{GeV}$ for almost the entire $0.2 \lesssim \Delta m_{\tilde{\chi}_1} \lesssim 3\,\mathrm{GeV}$ region except for a small sliver near $\Delta m_{\tilde{\chi}_1} \sim 0.2\,\mathrm{GeV}$. For a light sneutrino, DELPHI ran only exclude $m_{\tilde{\chi}_1^\pm} \lesssim 50-55\,\mathrm{MeV}$ for $0.5 \lesssim \Delta m_{\tilde{\chi}_1} \lesssim 3\,\mathrm{GeV}$, leaving a window from 0.05–0.5 GeV where the only lower limit is that from LEPI, 45 GeV. The gaps arise because of the low efficiency for detecting very soft pions.[2] In scenario (2), there is no gap where the best limit is that from LEPI. The CERN Intersecting Storage Rings (ISR) signature excludes $m_{\tilde{\chi}_1^\pm} \lesssim 58\,\mathrm{GeV}$ for $0.2 \lesssim \Delta m_{\tilde{\chi}_1} \lesssim 1\,\mathrm{GeV}$ and $m_{\tilde{\chi}_1^\pm} \lesssim 56\,\mathrm{GeV}$ for $1 \lesssim \Delta m_{\tilde{\chi}_1} \lesssim 3\,\mathrm{GeV}$.

Thus, in the $|M_2| < |M_1| \ll \mu$ scenario (1) on which we shall focus, depending on the sneutrino mass there may be a gap region in which the chargino is effectively invisible. DELPHI finds that the $\gamma\not{M}$ signature, discussed earlier, is indeed insufficient to improve over the $m_{\tilde{\chi}_1^\pm} \gtrsim 45\,\mathrm{GeV}$ limit from Z decays. We are uncertain whether DELPHI explored the use of high-impact-parameter tracks in their vertex detector (in association with the ISR trigger) to improve their sensitivity (by sharply reducing the $\gamma\nu\bar{\nu}$ background) in these gap regions.

B. Hadron colliders

At hadron colliders, typical signatures of MSUGRA are trilepton events from neutralino-chargino production, like-sign dileptons from gluino pair production, and multijets $+\not{E}_T$ from squark and gluino production. The trilepton signal from $\tilde{\chi}_1^\pm\tilde{\chi}_2^0$ production and the like-sign dilepton signal from $\tilde{g}\tilde{g}$ production are both suppressed when $\Delta m_{\tilde{\chi}_1}$ is small by the softness of the leptons coming from the $\tilde{\chi}_1^\pm$ decay(s). In $M_2 < M_1 \ll |\mu|$ scenarios, the trilepton signal is further diminished by the suppression of the $\tilde{\chi}_1^\pm\tilde{\chi}_2^0$ cross section. In $|\mu| \ll M_2, M_1$ scenarios, $m_{\tilde{\chi}_2^0} \simeq m_{\tilde{\chi}_1^0}$ and even though the $\tilde{\chi}_1^\pm\tilde{\chi}_2^0$ cross section is not suppressed the $\tilde{\chi}_2^0$ decay products, like those of the $\tilde{\chi}_1^\pm$, are very soft, yielding further suppression of the trilepton signal. Provided that $m_{\tilde{g}}$ is light enough, the most obvious signal for SUSY in degenerate models is jet(s) plus missing energy. Even if the gluino is rather degenerate with the $\tilde{\chi}_1^\pm$ and $\tilde{\chi}_1^0$, it has been shown [4] (see also [1]) that the Fermilab Tevatron and CERN Large Hadron Collider (LHC) will probe a significant (albeit reduced compared to MSUGRA boundary conditions) range of $m_{\tilde{g}}$. This is true since initial-state gluon radiation can be used to ''tag'' the missing energy. This search can also be augmented by the $\gamma\tilde{g}\tilde{g}$ process, where the γ is the tag. As $m_{\tilde{g}} - m_{\tilde{\chi}_1^\pm}$ increases, the jets from $\tilde{g} \to q\bar{q}\tilde{\chi}_1^\pm + q\bar{q}\tilde{\chi}_1^0$ decays become visible and the jet(s)$+\not{E}_T$ signature initially becomes stronger [4] despite the decrease in the $\tilde{g}\tilde{g}$ production cross section. However, it is entirely possible that the gluino is much heavier than the light $\tilde{\chi}_1^\pm, \tilde{\chi}_1^0$ states and that the $\tilde{g}\tilde{g}$ production rate (at the Tevatron at least) will be quite suppressed. In this case, the ability to detect events in which the only directly produced SUSY particles are light neutralino and chargino states could prove critical. In the remainder of this paper, we consider the sfermion, and heavier chargino and neutralino states to be extremely heavy, and investigate methods to probe degenerate models at the Tevatron. Expectations for scenarios where the gluino has a mass comparable to $\tilde{\chi}_1^\pm$ will be given less discussion. First, we study whether photon tagging (which we noted above is useful at a lepton collider) or jet tagging (as employed in many studies) might provide a viable signal when the $\tilde{\chi}_1^\pm$ decay is effectively prompt and its decay products are too soft to be visible in the detector. Later, we consider the modifications to this picture when the $\tilde{\chi}_1^\pm$ decay is not prompt.

For numerical estimates of signal and background rates, we perform particle level studies using either the processes contained in the PYTHIA 6.125 [15] event generator or by adding external processes (several of the $\gamma+$sparticles processes considered here) into PYTHIA. Signals involving chargino-neutralino pair production with jets are simulated using the tree-level chargino-neutralino pair process and parton showering. Based on our understanding of W and Z boson production at hadron colliders, this approach is more accurate than a matrix element calculation of chargino-neutralino production plus parton whenever the transverse momentum Q_T of the chargino-neutralino pair is less than the relevant hard scale Q. Here, that scale is $Q = \sqrt{s} > 2m_{\tilde{\chi}_1^\pm}$, and most of the data would lie below this scale. The estimates here are conservative, because they do not include the very high Q_T contribution ($Q_T > Q$) from chargino-neutralino pair plus one hard jet, nor the change of rate to the tree-level level process.

To determine experimental quantities, a calorimeter is defined out to $\eta = 4.4$ with a Gaussian E_T resolution of $\sigma_{E_T} = 80\%/\sqrt{E_T}$. Jets with $E_T > 5\,\mathrm{GeV}$ and $R = 0.5$ are recon-

[2]With the ISR tag, the $\gamma\gamma$ background is completely negligible.

structed to define $\not{E}_T$. Non-Gaussian contributions will be estimated as described later. Charged track momenta and impact parameters b are unsmeared, but the effects of detector resolution on b are included.

1. Pure γ or jet and $\not{E}_T$ signatures

One of the most challenging possibilities in degenerate models is when the $\tilde{\chi}_1^\pm$ decay is prompt and its decay products are too soft to be visible. At leading order in perturbation theory, $\tilde{\chi}_1^\pm(\to\tilde{\chi}_1^0+\text{soft})\tilde{\chi}_1^0$ and $\tilde{\chi}_1^+(\to\tilde{\chi}_1^0+\text{soft})\tilde{\chi}_1^-(\to\tilde{\chi}_1^0+\text{soft})$ production provide no good signature since the missing transverse momenta of the LSP's essentially cancels and the soft decay products are obscured by detector resolution and the combined effect of the underlying event and fragmentation-hadronization. However, it may still be possible to observe the transverse momentum of the LSP's if a high-p_T jet or photon is also produced in an event.

In the absence of mismeasurements, the major physics background to $\gamma+\not{E}_T$ at the Tevatron is $\gamma Z(\to\nu\overline{\nu})$ and $\gamma\tau^\pm\nu_\tau$ production, where $\tau(\to\not{E}_T+\text{soft})$. In reality, mismeasurements of jets can produce a false $\not{E}_T$, and the loss of a track can cause an electron to fake a photon. We can gain some insight into the relative importance of mismeasurement backgrounds from Run I analyses. The DØ Run I measurement of the $\gamma Z(\to\nu\overline{\nu})$ signal [16] (which is a background to our signature) has a background from $W(\to e^\pm\nu_e)$ when the e fakes a γ. For Run I the fake probability was roughly a constant with magnitude $R_{e\to\gamma}=5\times10^{-3}$. The background estimate in the DØ analysis is well reproduced by generating $W(\to e^\pm\nu_e)$ events with PYTHIA, replacing the e with a γ, weighting the event by an additional factor $R_{e\to\gamma}$, and performing all other cuts. The value of S/B is about 0.3, but the W contribution becomes negligible once $p_T^\gamma\gtrsim 50-60\,\text{GeV}$, which is beyond the Jacobian peak for the electron p_T spectrum. Another significant background arises from $\gamma+$jet, where the jet fakes $\not{E}_T$. For $\not{E}_T>40\,\text{GeV}$, this probability can be conservatively estimated[3] at $R_{j\to\not{E}_T}=10^{-4}$ [17]. This background can also be reproduced by generating $\gamma+q,\gamma+g$ events with PYTHIA, demanding only one reconstructed jet with $E_T>15\,\text{GeV}$, discarding this jet, weighting the event by an additional factor $R_{j\to\not{E}_T}$, calculating $\not{E}_T$ from the sum of all remaining jets, and performing all remaining cuts. Once $\not{E}_T>50\,\text{GeV}$, this background is roughly 5% of the $\gamma Z(\to\nu\overline{\nu})$ signal, and decreases quickly with increasing $\not{E}_T$. Since we can reproduce the mismeasurement backgrounds in a simple manner, we feel confident that we can reasonably estimate the full background. Additionally, we will set our cuts so that the mismeasurement backgrounds are smaller than the physics ones, which, for the chargino signal, will be dominated by $\gamma Z(\to\nu\overline{\nu})$. To reflect the detector improvements in Run II, we use the factor $R_{e\to\gamma}=10^{-3}$ [17].

To evaluate the viability of a $\gamma+\not{E}_T$ signature in degenerate scenarios, we have studied $\gamma\tilde{\chi}_1^+\tilde{\chi}_1^-$ and $\gamma\tilde{\chi}_1^+\tilde{\chi}_1^0$ production (computed for various values of M_2 taking $M_1=1.5M_2$, $\tan\beta=5$ and $\mu=1$ TeV—typically, $m_{\tilde{\chi}_1^\pm}\simeq m_{\tilde{\chi}_1^0}$ is close to M_2). Because only $\not{E}_T$ (and not $\not{E}$) can be measured, we cannot perform a cut that eliminates the real Z background from γZ production as can be done at LEP. At best, the distributions for signal and background in E_T^γ may be sufficiently different that a cut requiring high E_T^γ will allow a reasonable signal-to-background ratio, while retaining an adequate cross section for the signal. To demonstrate this, we plot in Fig. 2(a) the $\gamma\tilde{\chi}_1^+\tilde{\chi}_1^-$ and $\gamma\tilde{\chi}_1^\pm\tilde{\chi}_1^0$ integrated signal and $\gamma+\not{E}_T$ background (and some components thereof) as a function of a minimum accepted value for E_T^γ. (Note that the signal is multiplied by a factor of 10 in the figure.) Our nominal cuts are

$$E_T^\gamma>E_T^{\min},\ E_T>E_T^{\min},\quad |\eta^\gamma|<2.0,$$

$$\text{no jets with } E_T>15\ \text{GeV},\quad |\eta|<3.5,$$

$$\text{no } e\text{'s or } \mu\text{'s with } p_T>5\,\text{GeV},\quad |\eta|<2.0. \quad (2.1)$$

While the signal is somewhat flatter, $S/B>0.1$ is only achieved if a very high $E_T^{\min}$ cut is imposed, but then there are too few signal events. If $S/B\lesssim 0.1$ is required, the $\gamma+\not{E}_T$ signal can probe only $m_{\tilde{\chi}_1^\pm}\lesssim 50\,\text{GeV}$; $m_{\tilde{\chi}_1^\pm}\sim 60\,\text{GeV}$ can be probed only if systematics are understood at the $S/B\sim 0.05$ level. Either value is only a marginal improvement over the 45 GeV lower bound deriving from LEP Z-pole data. Even more importantly, both values are below the limits set by DELPHI (unless the sneutrino is light). In scenario (2), the signal cross section sum will be somewhat smaller than in scenario (1), and S/B will typically be too small to extract a signal from the data.

Given the importance of achieving a very small systematic error level in order to extend the LEP-LEP2 limits on an invisibly decaying chargino, it is worth noting that systematic errors do decrease with integrated luminosity, and many Run I analyses have systematic errors that are smaller than or the same size as the statistical error. The Run II situation should be much better than in Run I. Furthermore, we have not exploited any difference in shape between the signal and background, which may increase the significance of the signal. If any other distinguishing characteristics of the signal can be observed, or if there are other sources of chargino production, then the upper limit of $m_{\tilde{\chi}_1^\pm}$ for which the $\gamma+\not{E}_T$ signature is viable could be significantly larger than estimated here.

Given the somewhat pessimistic results for the $\gamma+\not{E}_T$ signal, it is worth exploring the standard SUSY jets$+\not{E}_T$ signal, which will have a larger event rate for comparable cuts. As compared to the normal MSUGRA scenario, the softness of the $\tilde{\chi}_1^\pm$ decay products implies that the jets$+\tilde{\chi}_1^+\tilde{\chi}_1^-$ events

[3]Note that $R_{j\to\not{E}_T}$ represents a non-Gaussian component to the $\not{E}_T$ resolution; the Gaussian component is already included in our calorimeter simulation.

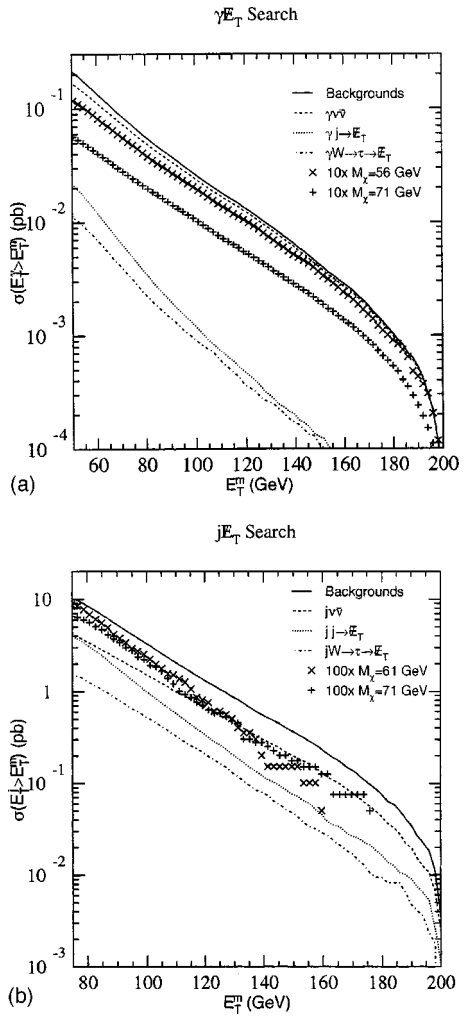

FIG. 2. Comparison of the signal and backgrounds for $\gamma+\not{E}_T$ and $j+\not{E}_T$ searches at the Tevatron for $\sqrt{s}=2$ TeV. In (a), we plot the sum of the $\gamma\tilde{\chi}_1^+\tilde{\chi}_1^-$ and $\gamma\tilde{\chi}_1^\pm\tilde{\chi}_1^0$ cross sections integrated over $E_T^\gamma, \not{E}_T > E_T^{\min}$, the additional cuts imposed are given in Eq. (2.1). Results are given for $m_{\tilde{\chi}_1^\pm} \simeq m_{\tilde{\chi}_1^0} \sim 56$ GeV and ~ 71 GeV; the signal has been multiplied by a factor of 10. In (b), we plot the $j\tilde{\chi}_1^+\tilde{\chi}_1^-$ and $j\tilde{\chi}_1^\pm\tilde{\chi}_1^0$ ''monojet'' cross sections integrated over $E_T^j, \not{E}_T > E_T^{\min}$, after imposing the additional cuts given in Eq. (2.2). Results are presented for $m_{\tilde{\chi}_1^\pm} \simeq m_{\tilde{\chi}_1^0} \sim 61$ GeV and ~ 71 GeV; the signal has been multiplied by a factor of 100.

will have much lower jet multiplicity. After including the effects of initial-state gluon radiation, many events have a monojet nature. The published Run I analyses have taken advantage of the jet multiplicity to control the QCD backgrounds, and are of little help in understanding potentially large monojet backgrounds. Thus, we will consider applying the standard MSUGRA 3-jet$+\not{E}_T$ cuts to a Monte Carlo prediction of the signal, using the published background estimates to set limits. Since the parton showering machinery can generate several jets per event, some signal events will pass the cuts. However, as discussed below, we find that there are substantial uncertainties in the Monte Carlo predictions for the multijet signal rate when the multiple jets are generated from parton showering and not by sparticle decays. Thus, we also consider a monojet signature for which we believe that the monojet$+\not{E}_T$ Monte Carlo signal rate computed using parton showering will be more reliable. This necessitates a study of the mismeasurement background. As discussed below, we believe that this and other monojet $+\not{E}_T$ backgrounds can be understood and convincingly controlled.

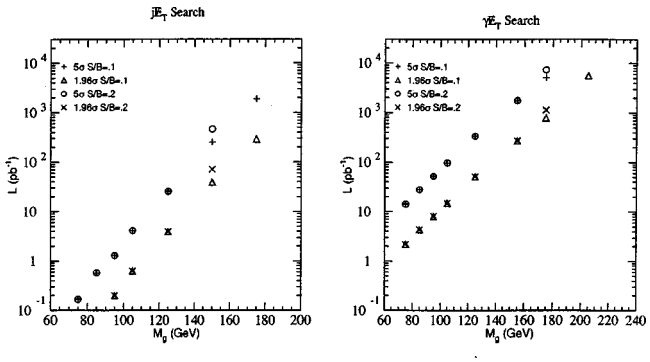

FIG. 3. Integrated luminosity (in pb^{-1}) required to observe ($S/\sqrt{B}=5$) or exclude at 95% CL ($S/\sqrt{B}=1.96$) a monojet$+\not{E}_T$ or $\gamma+\not{E}_T$ signal from $\tilde{g}\tilde{g}$ production, when $m_{\tilde{g}} \simeq m_{\tilde{\chi}_1^+}$. Predictions are shown for signal-to-background ratios of 0.1 and 0.2. For $m_{\tilde{g}}$ values above those for which points are plotted, S/B is below the required value. For the monojet$+\not{E}_T$[$\gamma+\not{E}_T$] signal we impose the cuts of Eq. (2.2) [Eq. (2.1)], optimizing $S/\sqrt{B}$ by scanning over $E_T^{\min}$ >75 GeV [>50 GeV].

We consider the monojet$+\not{E}_T$ signal first. To illustrate the size of the signal from jets$+\tilde{\chi}_1^+\tilde{\chi}_1^-$ and jets$+\tilde{\chi}_1^+\tilde{\chi}_1^0$ compared to background, we proceed much as in the case of the γ tag. Our specific cuts are

$$E_T^j > E_T^{\min}, \quad \not{E}_T > E_T^{\min}, \quad |\eta^j| < 3.5,$$

$$\text{no other jets with } E_T > 15\,\text{GeV}, \quad |\eta| < 3.5,$$

$$\text{no } e's \text{ or } \mu's \text{ with } p_T > 5\,\text{GeV}, \quad |\eta| < 2.0. \quad (2.2)$$

With these cuts, the physics backgrounds from $j\nu\bar{\nu} \to j\not{E}_T$ and $jW(\to\tau\to\not{E}_T)$ are larger than the mismeasurement background, which is predominantly jet+jet production, where one jet fakes $\not{E}_T$. We will only consider values of $E_T^{\min}$ above 75 GeV, which means that $\not{E}_T$ will always be required to be above the threshold employed for the Run I multijet analyses. To estimate the mismeasurement background, we have generated all QCD two parton processes with PYTHIA, and retained only those events containing exactly one or two jets with $E_T > 15$ GeV. If there are two jets, we then randomly discard one of the two and weight the event by a factor $2 \times R_{j\to\not{E}_T}$. We then impose the cuts of Eq. (2.2). For $E_T^j > E_T^{\min} = 75$ GeV, we arrive at a cross section estimate of 4 pb. The dominant physics backgrounds, $Z(\to\nu\bar{\nu})+$jet and $W(\to\tau\nu_T)+$jet, contribute 4 and 1.6 pb for the same cuts (note, we are far beyond the Jacobian peak, so that $W(\to l\nu_l)+$no jet, where $l=e,\mu,\tau$, can be ignored). Thus, even if our estimate of the QCD background is off by

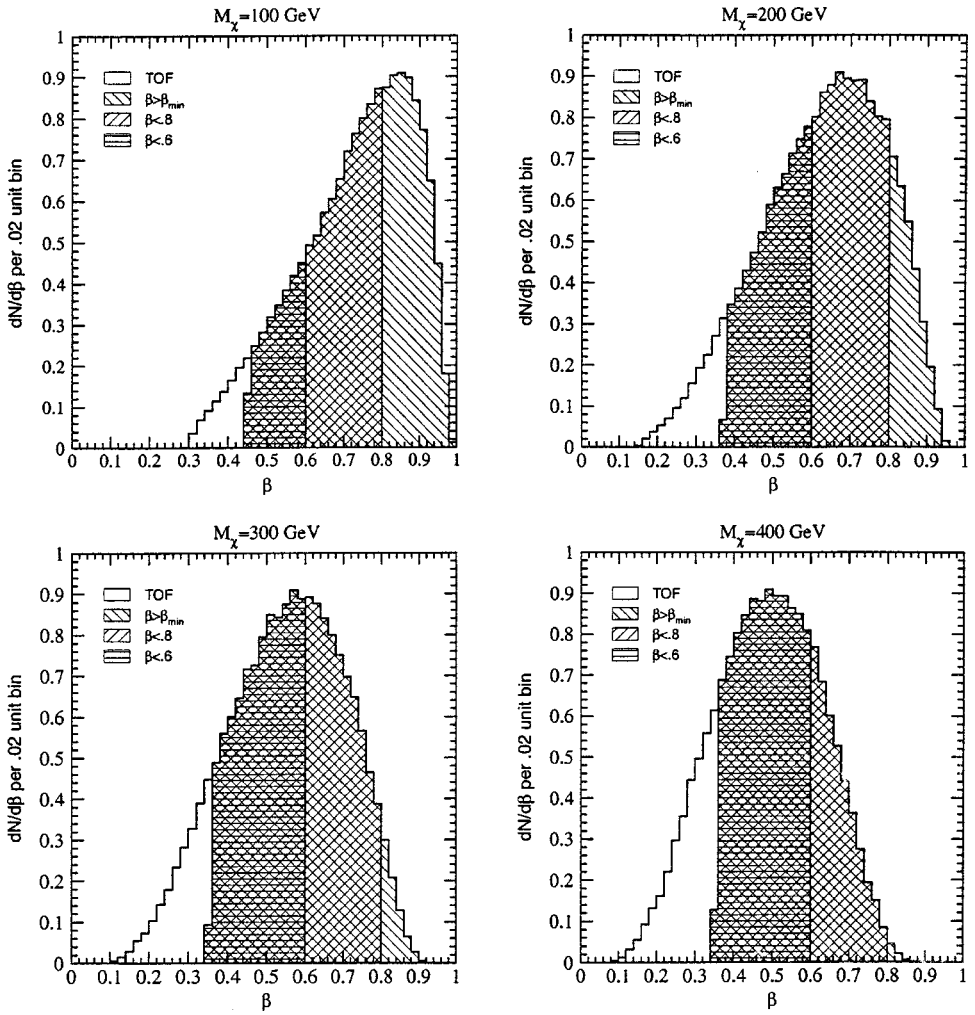

FIG. 4. Unnormalized β distributions for events accepted by the non-β cuts of Eq. (2.3) after requiring that the TOF time delay be >500 ps. The segments left after imposing various more restrictive β cuts are also shown. Distributions are given for $m_{\tilde{\chi}_1^\pm}=100$, 200, 300, and 400 GeV.

a factor of 2, this will not substantially bias an exclusion limit obtained using Gaussian statistics. After including $l\bar{l}$, single top, gauge boson pairs, and $W(\rightarrow e\nu_e,\mu\nu_\mu)+$jet backgrounds, the full background for the cuts of Eq. (2.2) and $E_T^{\rm min}=75$ GeV is about 10 pb.

Figure 2(b) shows the integrated cross section for the background and signal (signals are multiplied by 100 in the figure) as a function of $E_T^{\rm min}$. It is clear that the background is so severe that the monojet$+\not{E}_T$ channel will be much less useful than the $\gamma+\not{E}_T$ channel. To see if there is any hope for this discovery channel, we have varied the $E_T^{\rm min}$ cut in search of a value such that $S/B>0.1$ and such that there are at least 5 events for $L=30$ fb^{-1}. We never satisfy these constraints for $m_{\tilde{\chi}_1^\pm}>45$ GeV, so no limit beyond that from LEP Z-pole data can be set using this channel. Nonetheless, as explained below, a significant signal may appear in the $j+\not{E}_T$ channel if there are other sources of chargino production.

We will now turn momentarily to the multijet$+\not{E}_T$ signal. At the same time, we will also consider the more optimistic possibility that the gluino mass is small enough that $\tilde{g}\tilde{g}$ pair production has a reasonable rate at the Tevatron. In particular, we consider the limit, previously analyzed in Ref. [4] and motivated in the O-II model, that the gluino is almost degenerate in mass with the $\tilde{\chi}_1^\pm$. The results of Ref. [4] were that $m_{\tilde{g}}=150$ GeV could be excluded with $L=2$ fb^{-1} of data, and that this reach could not be extended using higher L if one demanded $S/B>0.2$. The exclusion was based on background estimates from DØ and CDF for their Run I 3 jet $+\not{E}_T$ searches. We have repeated the analysis of Ref. [4] using PYTHIA instead of ISAJET [18]. We find that we cannot reproduce all of the results of Ref. [4], and the reasons (to be discussed below) suggest that one may not wish to trust results obtained via Monte Carlo for a multijet$+\not{E}_T$ signal of the type considered here, in which the jets are generated entirely by parton showering. For example, consider $m_{\tilde{g}}=75$ GeV. Using PYTHIA, we find roughly half the signal cross section (compared to [4]) after the DØ cuts. This discrepancy arises because of the details of parton showering used in ISAJET (Ref. [4]) as compared to PYTHIA (our study). For the first, soft-gluon emission in a shower, PYTHIA restricts the polar angle of the branching to be smaller than the angle of the color flow, while ISAJET does not. As a result, the soft gluons in ISAJET are more widely distributed, and the resultant jet multiplicity is higher. Indeed, when we turn off the angular ordering effect in PYTHIA, we reproduce the ISAJET results. For larger $m_{\tilde{g}}$, however, the discrepancy re-

mains, and is not entirely resolved. If we use the PYTHIA results, the Ref. [4] Tevatron limit on $m_{\tilde{g}}$ is reduced to $m_{\tilde{g}} \sim 95-100\,\mathrm{GeV}$. However, the comparison of the two Monte Carlo programs suggests that one cannot trust a parton showering result in degenerate scenarios for three hard, well-separated jets.

Thus, we return to our proposed monojet signature to estimate the potential of the Tevatron for probing the $m_{\tilde{g}} \sim m_{\tilde{\chi}_1^\pm} \simeq m_{\tilde{\chi}_1^0}$ scenario. As already noted, the $\not\!\!E_T$ signature is enhanced by $q\bar{q},gg \to \tilde{g}\tilde{g}$, where $\tilde{g} \to q'\bar{q}\tilde{\chi}_1^\pm, q\bar{q}\tilde{\chi}_1^0$. For small $m_{\tilde{g}} - m_{\tilde{\chi}_1^\pm}$ the $q,q',\bar{q}$ are typically too soft to be counted as jets and the $\tilde{\chi}_1^\pm$ decay products are not visible. Thus, the monojet still comes from parton showering. In Fig. 3(a) we plot the luminosity required for $S/\sqrt{B}=1.96$ or 5 and $S/B > 0.1$ or 0.2 as a function of $m_{\tilde{g}}$. We have employed the cuts of Eq. (2.2), searching for the $E_T^{\min} > 75\,\mathrm{GeV}$ value that maximizes $S/\sqrt{B}$ while satisfying the given S/B criteria. (For lower $m_{\tilde{g}}$, $E_T^{\min}=75\,\mathrm{GeV}$ is always best; for the highest $m_{\tilde{g}}$ values the best $E_T^{\min}$ increases.) With the increased production of charginos and neutralinos from gluino decays, it is much easier to achieve $S/B > 0.2$ and a gluino with $m_{\tilde{g}} = 150\,\mathrm{GeV}$ should be discovered or excluded early in Run II. However, discovering or excluding $m_{\tilde{g}} = 175\,\mathrm{GeV}$ will require reducing systematics to the extent that an $S/B=0.1$ signal can be trusted. Specifically, for $S/B > 0.1$, $m_{\tilde{g}} = 175\,\mathrm{GeV}$ can be excluded at 95% CL with $L = 0.3\,\mathrm{fb}^{-1}$ or discovered at the 5σ level with $L = 2\,\mathrm{fb}^{-1}$.

The process $\gamma\tilde{g}\tilde{g}$, where $\tilde{g} \to$ soft, yielding a $\gamma + \not\!\!E_T$ signal, is complementary to the monojet$+\not\!\!E_T$ signal. We follow the same procedure as discussed for the monojet$+\not\!\!E_T$ signal, except that we employ the cuts of Eq. (2.1) and require $E_T^{\min} > 50\,\mathrm{GeV}$. The luminosity required to discover or exclude a given $m_{\tilde{g}}$ using this signal is plotted in Fig. 3(b). Even though the $\gamma + \not\!\!E_T$ signal requires more integrated luminosity to establish a signal for low $m_{\tilde{g}}$, S/B is larger, allowing exclusion out to a larger value of the common chargino/gluino mass; $m_{\tilde{\chi}_1^\pm} \sim m_{\tilde{g}} \lesssim 175\,\mathrm{GeV}$ can be excluded at 95% CL with $L = 1\,\mathrm{fb}^{-1}$ of integrated luminosity even if $S/B > 0.2$ is required.

For purposes of comparison, we note that in an MSUGRA scenario the trilepton signature from $\tilde{\chi}_1^\pm \tilde{\chi}_2^0$ production allows one to probe chargino masses up to about 160 GeV for $L = 30\,\mathrm{fb}^{-1}$ when the scalar soft-SUSY-breaking mass is large [19].

We note that the monojet$+\not\!\!E_T$ and $\gamma + \not\!\!E_T$ signatures should persist (and perhaps even improve somewhat) for $m_{\tilde{g}} - m_{\tilde{\chi}_1^\pm} \sim \mathrm{few} - 10\,\mathrm{GeV}$ and/or $\Delta m_{\tilde{\chi}_1} \sim \mathrm{few} - 10\,\mathrm{GeV}$.

Before concluding this subsection, we should comment that there are potential contributions from $\tilde{g}\tilde{\chi}_1^\pm$ and $\tilde{g}\tilde{\chi}_1^0$ production that have not been included here. These are suppressed when the squark masses are large, as assumed here. For the remainder of the paper, we assume that the gluino is also very heavy.

2. LHIT and TOF signatures

In the previous section, we considered the case where the mass splitting was large enough for the chargino decay to be very prompt, but yet too small for the chargino decay products to be visible. In this section, we consider the opposite extreme, namely $\Delta m_{\tilde{\chi}_1}$ sufficiently small that the chargino is so long lived that it passes through the TOF and enters the muon chambers. For instance, if $\Delta m_{\tilde{\chi}_1} < m_\pi$, then the average $c\tau$ is of the order of a meter or more. Of course, as noted earlier, the radiatively generated mass splitting makes $\Delta m_{\tilde{\chi}_1} < m_\pi$ somewhat unlikely in existing models. But, even for $\Delta m_{\tilde{\chi}_1} > m_\pi$, there is a tail of events with large enough $\beta\gamma c\tau$ values for the chargino to reach the muon chambers. Thus, from the experimental point of view it is important to consider signals based on a muon-chamber LHIT or TOF signal as a function of $\Delta m_{\tilde{\chi}_1}$.

To distinguish a chargino that reaches the muon chambers from an actual muon without using the TOF, we employ the procedures used by CDF in Run I for identifying a penetrating particle that is sufficiently heavily ionizing that it cannot be a muon. However, because the DØ inner muon chambers are closer to the interaction point and cover more range in $|\eta|$, it is advantageous to employ the DØ muon chamber configuration (see earlier description). In analogy to the CDF Run I procedure, we first demand a trigger for the event using one track (Track I) that penetrates to the muon chambers. We then examine the triggered events for a track (Track II) that is heavily ionizing and penetrates to the muon chambers. The specific LHIT cuts/requirements we impose in our study are[4]

$$\begin{aligned} &\text{Tracks I and II:} \quad (|\eta|<1, \beta_\perp \gamma c\tau > 2.7\,\mathrm{m}) \\ &\qquad \text{or } (1<|\eta|<2, |\beta_z|\gamma c\tau > 4\,\mathrm{m}),\ \beta > \beta_{\min}, \\ &\text{Track I:} \quad p_T > 15\,\mathrm{GeV}, \\ &\text{Track II:} \quad |\vec{p}| > 35\,\mathrm{GeV},\ \beta_\gamma < 0.85, \end{aligned} \tag{2.3}$$

where $\beta_{\min}$ is the minimum velocity required for the $\tilde{\chi}_1^\pm$ to penetrate to the muon chambers. $\beta_{\min}$ varies with $m_{\tilde{\chi}_1^\pm}$, and is calculated using the model employed in Ref. [20]. In Eq. (2.3), $\beta_\perp$ is the velocity perpendicular to the side of the box formed by the inner muon chambers (see earlier description) that the chargino eventually passes through, and $\beta\gamma < 0.85$ is the 2MIP requirement. Tracks I and II may be the same track. LHIT events are expected to be background free.

For small $m_{\tilde{\chi}_1^\pm}$, the $\tilde{\chi}_1^\pm \tilde{\chi}_1^0$ and $\tilde{\chi}_1^+ \tilde{\chi}_1^-$ production cross sections are large before cuts, but the $\beta_{\min}$ and $\beta\gamma$ requirements accept only a small portion of the full rate. For larger $m_{\tilde{\chi}_1^+}$, the cross section decreases, but $\beta\gamma$ is typically smaller. These trends are illustrated in Fig. 4. This figure shows the full β distributions for $m_{\tilde{\chi}_1^\pm} = 100$, 200, 300, and 400 GeV that remain after requiring that the chargino pass through the

[4]Note that since the CDF procedure was originally designed for looking for massive quarks, they did not impose a requirement of small hadronic energy deposit in the track direction(s). We have not imposed this requirement either. However, for the chargino signal of interest here it could be imposed with little loss of signal event rate were this useful for reducing backgrounds.

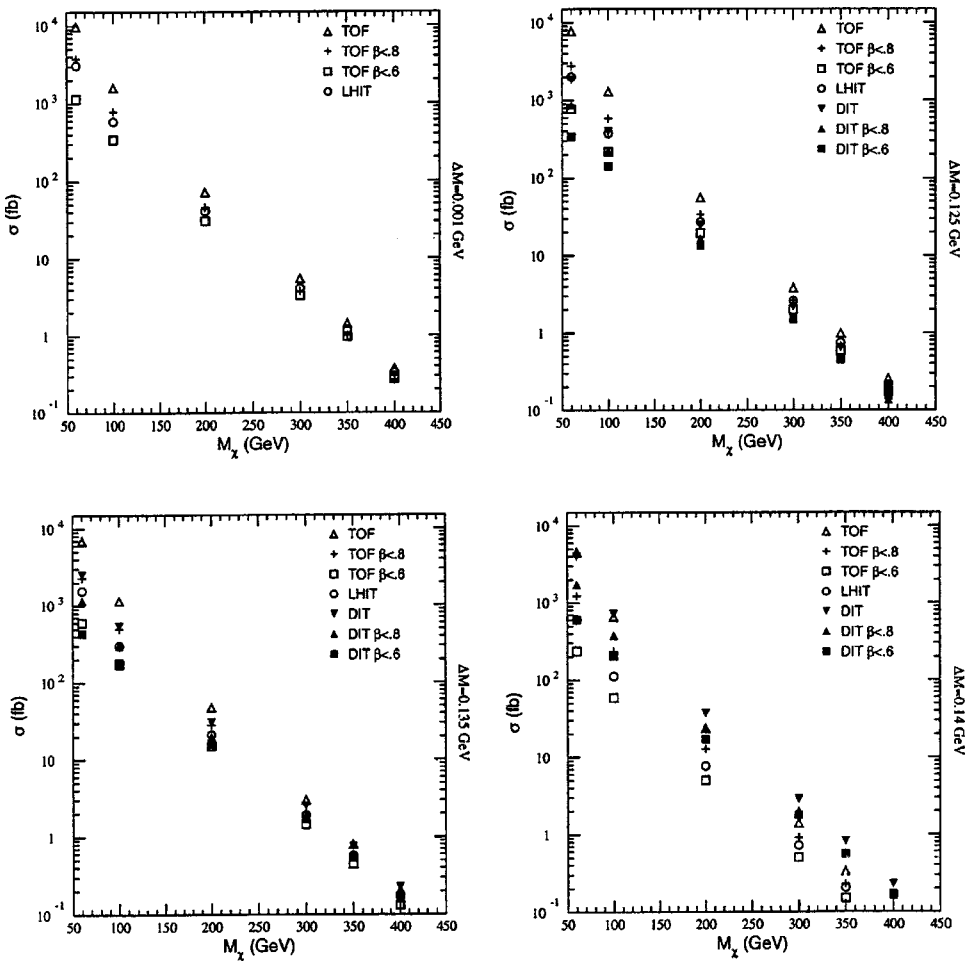

FIG. 5. Cross sections for LHIT, TOF, and DIT ''background-free'' signatures at Run II: $\Delta m_{\tilde{\chi}_1}=0$, 125, 135, 140 MeV.

TOF device at least 500 ps later than a particle with $\beta=1$ (as required in the TOF signal discussed below). The impact of the $\beta_{\min}$ cut and of various requirements on the maximum value of β is also shown. We see that for $m_{\tilde{\chi}_1^\pm}=100\,\mathrm{GeV}$ a relatively small slice of the β distribution is retained after requiring both $\beta>\beta_{\min}$ and $\beta<0.6(\beta\gamma<0.75)$ or $\beta<0.65(\beta\gamma<0.85)$. The slice accepted by such cuts is much larger for $m_{\tilde{\chi}_1^\pm}=400\,\mathrm{GeV}$.

The cross section obtained after imposing all the cuts of Eq. (2.3) is plotted as the open circles in Fig. 5 for a selection of $\Delta m_{\tilde{\chi}_1}$ values. For $c\tau=\infty$, $m_{\tilde{\chi}_1^+}=350\,\mathrm{GeV}$ (450 GeV) can be excluded at the 95% C.L. (three events predicted, none observed) with 2 (30) fb^{-1} of data. A five-event discovery would require $m_{\tilde{\chi}_1^\pm}\leqslant 325\,\mathrm{GeV}$ ($\leqslant$430 GeV) for $L=2\,\mathrm{fb}^{-1}$ (30 fb^{-1}). The three event limits for various $\Delta m_{\tilde{\chi}_1}$ values are summarized in Fig. 12. As expected, the LHIT signal mass reach declines as $\Delta m_{\tilde{\chi}_1}$ increases, and the LHIT signal has vanished by $\Delta m_{\tilde{\chi}_1}=142.5\,\mathrm{MeV}$.

The time-of-flight (TOF) signal is defined similarly to the LHIT signal, except that the $\beta\gamma<0.85$ requirement is replaced by the requirement that Track II arrive at the TOF device at least 500 ps later than would a relativistic track. For the expected 100 ps time resolution of the TOF signal, this corresponds to a 5σ delay in arrival compared to a particle with $\beta\sim 1$. Thus, we replace the $\beta\gamma<0.85$ requirement by

$$d_{\mathrm{TOF}}/(\beta c)-d_{\mathrm{TOF}}/c>500\,\mathrm{ps}, \tag{2.4}$$

where d_{TOF} is the distance to the muon chamber along the direction of flight.

As mentioned previously, for smaller $m_{\tilde{\chi}_1^\pm}$ values the TOF signal accepts a significantly larger range of $\beta\gamma$ than does the heavy-ionization $\beta\gamma<0.85$ requirement of the LHIT signal. This is apparent from the $m_{\tilde{\chi}_1^\pm}=100$ and 200 GeV windows of Fig. 4 by comparing the total $\beta>\beta_{\min}$ region to the $\beta_{\min}<\beta<0.65$ region. However, for large $m_{\tilde{\chi}_1^\pm}$ near the upper limit that can be probed by the LHIT signal (see the $m_{\tilde{\chi}_1^\pm}=400\,\mathrm{GeV}$ window of Fig. 4) the $\beta<0.65$ ($\beta\gamma<0.85$) LHIT cut has similar efficiency to the TOF cut. Thus, we can anticipate that the TOF signal will be viable for lower luminosity than the LHIT signal if $m_{\tilde{\chi}_1^\pm}$ is not large, but that the TOF signal will not be viable for $m_{\tilde{\chi}_1^\pm}$ values much beyond those reachable by the LHIT signal.

The TOF cross sections as a function of $m_{\tilde{\chi}_1^\pm}$ are given in Fig. 5 for the same $\Delta m_{\tilde{\chi}_1}$ values for which the LHIT cross sections were plotted. As expected, Fig. 5 shows that the TOF signal is much more efficient than the LHIT signal at lower masses, but the upper mass limit attained using the TOF and LHIT signals is the same, e.g., $m_{\tilde{\chi}_1^\pm}\sim 430\,\mathrm{GeV}$ for $L=30\,\mathrm{fb}^{-1}$ and $\Delta m_{\tilde{\chi}_1}=125\,\mathrm{MeV}$.

The underlying reason that the TOF and LHIT upper mass limits are the same is due to the *s*-wave nature of the $\tilde{\chi}_1^+\tilde{\chi}_1^-$ and $\tilde{\chi}_1^\pm\tilde{\chi}_1^0$ production subprocesses, which, in turn, implies large cross sections in $p\bar{p}$ collisions out to high $m_{\tilde{\chi}_1^\pm}$. This can be contrasted with the result for long-lived staus. The *p*-wave nature of the $\tilde{\tau}^+\tilde{\tau}^-$ production subprocesses implies much smaller $p\bar{p}$ cross sections, for which the LHIT signal mass reach is limited to $m_{\tilde{\tau}} \lesssim 145\,\text{GeV}$. For such masses, the LHIT requirement of $\beta\gamma < 0.85$ is very restrictive. Due to its acceptance of $\beta\gamma$ values substantially beyond 0.85, the TOF signal improves the mass reach to 175 GeV [13].

As a final comment, we believe that the presence of an additional TOF device between the EC and HC could be of significant value in the search for $c\tau \lesssim 1$ m. With an appropriate electronics design, events with a chargino that reached the inner TOF device but not the muon chamber could be triggered by the inner TOF signal and the presence of a stiff chargino track in the tracker. The time delay of the TOF signal would indicate the mass of the particle, and such events would be background free. However, the mass reach would only improve over the DIT signal discussed below if a heavy-ionization requirement has to be imposed in order that the latter be background free.

3. DIT signatures

As $\Delta m_{\tilde{\chi}_1}$ increases above m_π, $c\tau$ becomes too small to produce a LHIT or TOF signature with large efficiency. The next signature of interest is an isolated track that passes all the way through the CT but disappears before reaching the TOF and MC. The disappearing, isolated track signature is denoted by DIT. For our study, we employ the DØ detector CT radius of 73 cm (which gives greater coverage for this signal than does the CDF detector with CT radius of 130 cm). The DØ trigger logic is well adapted to this type of signal in that the CT track itself can be used to trigger the event provided it is sufficiently isolated. The isolation required by DØ for a track trigger is that no other track be in the same azimuthal wedge as the trigger track. Each azimuthal wedge is of size $\Delta\phi \sim 0.1$. The specific DIT triggering requirements we impose are

$$\beta_T \gamma c\tau > 73\,\text{cm},$$

$$p_T^{\text{trigger}} > 11\,\text{GeV}, \quad |\eta^{\text{trigger}}| < 2,$$

$$\sum_{|\Delta\phi|<0.1} p_T^{\text{tracks}} - p_T^{\text{trigger}} < 2\,\text{GeV}, \tag{2.5}$$

where $\Delta\phi = \phi^{\text{track}} - \phi^{\text{trigger}}$ [17]. Once the event is triggered, we require (off-line) that it have high p_T and decay before reaching the TOF device and the muon chamber. Without this latter requirement, the track would be confused with a muon, unless we impose a further requirement that it be heavily ionizing. We hope to avoid such a requirement as it significantly reduces the signal event rate. Our specific DIT cuts are then

$$p_T^{\text{track}} > 30\,\text{GeV}, \quad 73\,\text{cm} < \beta\gamma c\tau < d_{\text{TOF}}, \quad E_{\text{cal}}(\Delta R < 0.4) - E_{\text{cal}}^{\tilde{\chi}_1^\pm}(\beta) \lesssim 2\,\text{GeV}, \tag{2.6}$$

where d_{TOF} is the distance to the TOF device, e.g., to the box of the inner DØ muon chamber, $E_{\text{cal}}(\Delta R < 0.4)$ is the total energy deposited in the EC and HC calorimeters in the indicated cone surrounding the track, and $E_{\text{cal}}^{\tilde{\chi}_1^\pm}(\beta)$ is the average ionization energy that the chargino would be expected to deposit in the EC and HC calorimeters for its (measured) β in the given event, assuming it does not decay before exiting the HC. Given that in some events the chargino will decay soon after entering the EC, this latter cut is quite conservative. A more optimal approach when the calorimeters are sufficiently segmented in the radial direction might be to look for events with chargino ionization energy deposits in a few inner segments but no corresponding energy deposits along the track direction in the outer segments. If the termination of the track could be seen despite the small size of the ionization energy deposits (2–3 MIP's, typically) and if ''hot-spot''/K^0/ . . . backgrounds are not large, such events would be clearly distinct from background events, especially given the $p_T^{\text{track}} > 30\,\text{GeV}$ cut. We have not attempted to implement this approach in our studies. In the absence of using the radial segmentation, the E_{cal} cut may be very important for eliminating backgrounds. Fortunately, it is highly efficient for the signal. Although, $\tilde{\chi}_1^\pm\tilde{\chi}_1^0$ and $\tilde{\chi}_1^+\tilde{\chi}_1^-$ production will have the usual hadronic (initial-state radiation, minijet, . . .) activity associated with a hard scattering event, the probability of having more than 5 GeV of E_T of such activity in $|\eta| < 1$ is only about 30%, implying that small E_{cal} near the chargino, in addition to the ionization energy deposits of the chargino itself, will be automatic for most signal events.

As discussed earlier, the requirements of Eq. (2.6) may on their own be sufficient to yield a background-free signal. In this regard, the $E_{\text{cal}}(\Delta R < 0.4)$ cut is probably critical for eliminating backgrounds. For example, an event in which a Σ^+ or Σ^- is produced and makes an isolated track in the tracker would be removed by this cut. Even if the $\Sigma^\pm$ decays just outside the central tracker, its decay products are strongly interacting and will produce substantial deposits in the calorimeters, especially the hadronic calorimeter. Still, even after the $E_{\text{cal}}(\Delta R < 0.4)$ cut, one should consider the possibility that the DIT signal will not be entirely free of background. If not, one can impose a heavy-ionization requirement. The ionization of the DIT will be measured in the SVX, CT, and PS. We will consider cuts requiring $\beta < 0.6$ ($\beta\gamma < 0.75$) or $\beta < 0.8$ ($\beta\gamma < 1.33$). The former is roughly equivalent to requiring three MIP's of ionization. As illustrated in Fig. 4, the latter is a much weaker cut that would accept many more signal events (at least for lower chargino masses), but we estimate that it would still reduce the number of background events containing 1MIP tracks by at least a factor of 10. The DIT signals with the above β cuts are denoted by DIT6 and DIT8.

Cross sections for the DIT, DIT6, and DIT8 signals are plotted as solid triangles, upside-down triangles and squares,

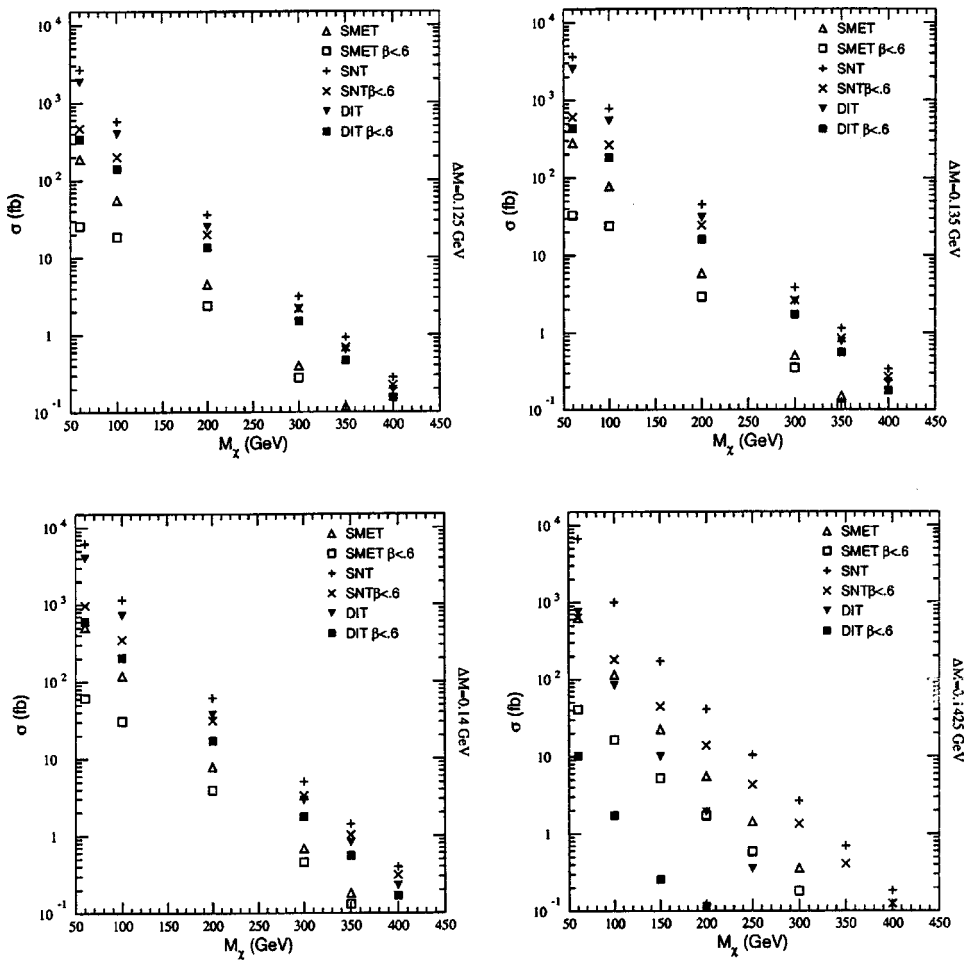

FIG. 6. Cross sections for DIT and STUB ''background-free'' signatures at Run II: $\Delta m_{\tilde{\chi}_1}=125$, 135, 140, 142.5 MeV.

respectively, in Figs. 5, 6, and 7. From Fig. 5, one finds that for $\Delta m_{\tilde{\chi}_1} > 125\,\mathrm{MeV}$ the DIT signal is as good or better than the LHIT signal. From the $\Delta m_{\tilde{\chi}_1}=140\,\mathrm{MeV}$ window of Fig. 5, we see that even the DIT6 signal becomes superior to the LHIT and TOF signals as soon as $\Delta m_{\tilde{\chi}_1}$ exceeds m_π. Figure 6 repeats some of the small $\Delta m_{\tilde{\chi}_1}$ DIT results, but now in comparison to the STUB and STUB+KINK signals discussed in the next section. Also shown in Fig. 6 is a $\Delta m_{\tilde{\chi}_1}=142.5\,\mathrm{MeV}$ window. One sees that the DIT signals survive crossing the $\tilde{\chi}_1^\pm \to \pi^\pm \tilde{\chi}_1^0$ decay threshold. In contrast, the LHIT and TOF cross sections are already very small at this $\Delta m_{\tilde{\chi}_1}$ value. Figure 7 gives results for the DIT signals for still larger $\Delta m_{\tilde{\chi}_1}$ values. Assuming no background, the 95% C.L. reaches of the DIT and DIT6 signals are given in Fig. 12 for a range of $\Delta m_{\tilde{\chi}_1}$ values using the three event (no background) criterion.

4. STUB and KINK signatures

As the chargino lifetime becomes still shorter, the probability for triggering an interesting event using LHIT, TOF or DIT signals becomes small. In this case, the $\not{E}_T$ generated by initial-state-radiation of jets can be used to trigger the event. Such jets are inevitably present in association with pair production of massive particles at a hadron collider. In this section, we will then identify a chargino event by looking for a track that passes all the way through the SVX but disappears prior to reaching the outer radius of the central tracker, i.e., a STUB track. The $c\tau$ range of interest is thus roughly $50\,\mathrm{cm} \gtrsim c\tau(\tilde{\chi}_1^\pm) \gtrsim$ few cm. From Fig. 1 and Table I, we observe that such $c\tau$ values are predicted as $\Delta m_{\tilde{\chi}_1}$ ranges from just slightly above m_π up to about 190 MeV. In this $\Delta m_{\tilde{\chi}_1}$ range, the chargino decays primarily to a single soft charged pion plus the $\tilde{\chi}_1^0$. The soft pion might be visible in the tracker (where it would be emitted at substantial angle relative to the STUB track, resulting in a KINK type of signature). The neutralino takes most of the energy of the decay and is invisible. There are no calorimeter deposits associated with the STUB. Thus, interesting events can potentially be identified by demanding that the STUB be heavily ionizing, be connected to a KINK, and/or have no associated calorimeter deposits.

For this study, we assume the detector capabilities and structure of the CDF detector, including the upgraded SVX described in Ref. [11]. We define a STUB track by the requirement that the chargino pass through all layers of the vertex detector (we assume that $L00$ is present) and that it have large p_T (as determined off-line using the SVX track). We also demand that there be very little calorimeter activity in a cone surrounding the STUB and that the track not make it to the end of the CT or, equivalently, to the PS (in particu-

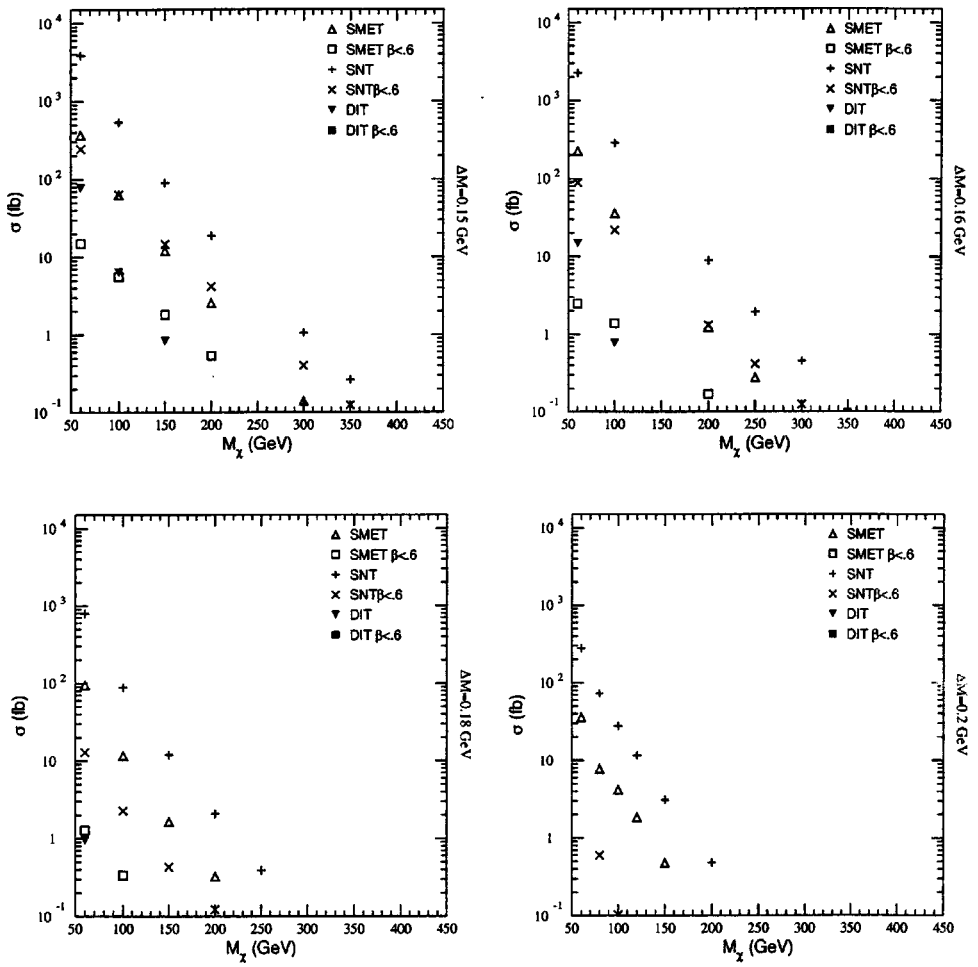

FIG. 7. Cross sections for DIT and STUB ''background-free'' signatures at Run II: $\Delta m_{\tilde{\chi}_1}=150$, 160, 180, 200 MeV.

lar, it does not enter the calorimeters). Our specific STUB requirements are

$$p_T>30\,\mathrm{GeV},\quad E_{\mathrm{cal}}(\Delta R<0.4)<2\ \mathrm{GeV},$$

$$\beta_T\gamma c\tau>11\,\mathrm{cm},\quad |\beta_z|\gamma c\tau<45\,\mathrm{cm},\quad \beta\gamma c\tau<d_{\mathrm{PS}}. \quad (2.7)$$

There is some chance that a signal requiring one or more STUB's might be background free, but such events cannot be triggered on in the present CDF and DØ designs by virtue of the fact that the SVX information is not analyzed until level 3. Still, should some sign of this scenario become apparent in Run II data, perhaps via a very weak DIT signal, an upgrade of the trigger to include this possibility might be feasible.

Additional handles are available for ensuring that a STUB signal is background free. First, one can search for the KINK created when the chargino responsible for the STUB decays to a charged pion inside the tracker. For $c\tau$ values near 11 cm, this will be very probable. We will not explicitly explore the efficiency for searching for KINK's here. However, we have computed STUB cross sections after requiring that the chargino decay a significant distance prior to reaching the outer radius of the CT. Specifically, we will give STUB cross sections for decay prior to a radial distance of 50 cm or 1.1 m. (The former is appropriate for the DØ tracker that ends at 73 cm—the latter is appropriate for the CDF tracker that extends to 1.3 m.) This type of signature will be denoted by SK (for STUB+KINK).

Finally, we have considered the additional requirement of heavy ionization deposit in the SVX. Thus, we also present results requiring $\geqslant$1 STUB with $\beta<0.6$. The $\geqslant$3 MIP ionization of a $\beta<0.6$ track, accompanied with the high p_T requirement and the lack of associated calorimeter activity would certainly make this a background-free signal. Note that the STUB requirement that the chargino pass through all six layers of the SVX is critical to obtaining enough dE/dx samples for a reliable determination of whether or not the track is heavily ionizing. Samplings from just a couple of layers would not be adequate.

Results for the cross sections obtained by requiring $\geqslant$1 STUB, possibly with $\beta<0.6$ imposed, and no additional trigger (NT), are denoted by SNT and SNT6, respectively. The cross sections for these signals as a function of $m_{\tilde{\chi}_1^\pm}$ are plotted in Figs. 6 and 7 for a series of $\Delta m_{\tilde{\chi}_1}\leqslant 200\,\mathrm{MeV}$ values. Of course, they are always larger than the DIT, DIT8, and DIT6 cross sections, and certainly remain substantial out to much larger $\Delta m_{\tilde{\chi}_1}$ values. The 95% C.L. limits based on three events (no background) are given for the SNT and SNT6 signals for a selection of $\Delta m_{\tilde{\chi}_1}$ values in Fig. 12. Here, we see very significant mass reach results for the

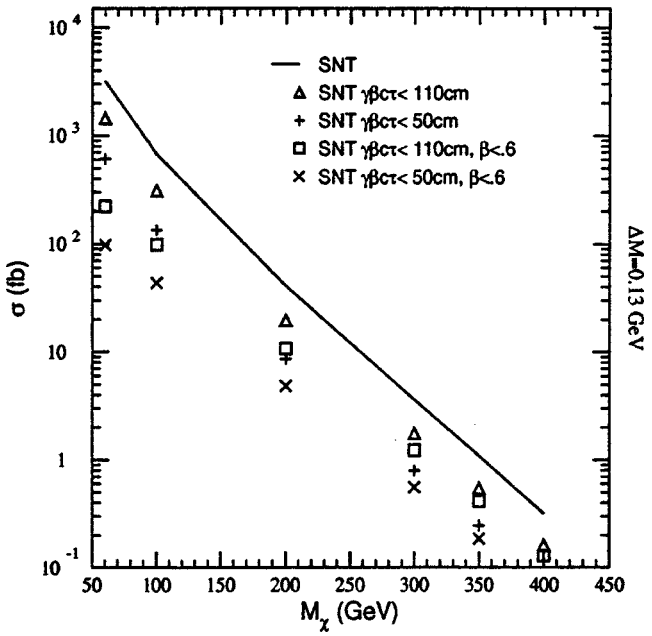

FIG. 8. Cross sections for SKNT and SKNT6 signals where the KINK distance is either 50 cm, as appropriate for D$\emptyset$, or 110 cm, as appropriate for CDF. The solid curve is the SNT (no β cut) cross section.

smallest of the $\Delta m_{\tilde{\chi}_1}$ values, but the mass reach decreases significantly as $\Delta m_{\tilde{\chi}_1}$ increases. In particular, we note that for $\Delta m_{\tilde{\chi}_1} \geqslant 250\,\mathrm{GeV}$, only the SNT signal (and the SMET signal discussed below) have cross sections above 0.1 fb for $m_{\tilde{\chi}_1^\pm} \geqslant 50\,\mathrm{GeV}$. The corresponding 95% CL upper limits are shown in Fig. 12, but we do not give the corresponding cross section plots.

In order to assess the efficiency for seeing KINK's in association with STUB's we present Figs. 8 and 9. In Fig. 8, we give $\Delta m_{\tilde{\chi}_1} = 130\,\mathrm{MeV}$ cross sections for the 50 and 110 cm maximum radii (as appropriate for D$\emptyset$ and CDF, respectively), both before and after a $\beta < 0.6$ cut, in comparison to the full SNT cross section (no β cut). For any $\Delta m_{\tilde{\chi}_1} < m_\pi$, the relative efficiencies for these different cross sections are essentially the same. But, observation of a KINK decay for $\Delta m_{\tilde{\chi}_1} < m_\pi$ will be very difficult since the electron in the dominant $\tilde{\chi}_1^\pm \to e^\pm \nu_e \tilde{\chi}_1^0$ decay is very soft. However, once $\Delta m_{\tilde{\chi}_1} > m_\pi$ we will be looking for a somewhat harder (but still soft) charged pion daughter track. In Fig. 9, we present the SKNT and SKNT6 cross sections for the D$\emptyset$ KINK distance of 50 cm for $\Delta m_{\tilde{\chi}_1} = 140\,\mathrm{MeV}$ and $\Delta m_{\tilde{\chi}_1} = 142.5\,\mathrm{MeV}$. We observe that the $\Delta m_{\tilde{\chi}_1} = 142.5\,\mathrm{MeV}$ SNT and SKNT results are essentially the same. This is because, for $\Delta m_{\tilde{\chi}_1} > 142.5\,\mathrm{MeV}$, the $c\tau$ of the $\tilde{\chi}_1^\pm$ is sufficiently short that the decay always occurs before reaching 50 cm. Similarly, results for the CDF KINK distance of 1.1 m differ very little from the SNT results for any $\Delta m_{\tilde{\chi}_1} \geqslant 140\,\mathrm{MeV}$.

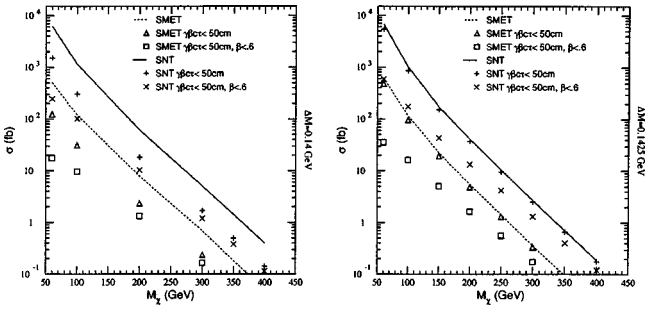

FIG. 9. Cross sections for SKNT, SKNT6, SKMET, and SKMET6 signals at D$\emptyset$ in which the K refers to the requirement that the chargino decay prior to a radial distance of 50 cm. Also shown for comparison, as the solid and dotted lines, respectively, are the SNT and SMET (no β cut) cross sections at D$\emptyset$.

Unfortunately, as we have already emphasized, the above signals are not available for the current CDF and D$\emptyset$ trigger designs. Thus, we now consider STUB and STUB+KINK type signatures using an $\not{E}_T > 35\,\mathrm{GeV}$ trigger for the event ($\not{E}_T$ is computed assuming $|\eta| < 4$ calorimeter coverage and standard smearing and without including any SVX or tracker information). These signals will be generically denoted by SMET and SKMET. The $\not{E}_T$ trigger selects events with initial-state gluon radiation. For reference, the $\not{E}_T > 35\,\mathrm{GeV}$ trigger requirement retains 8–13 % of all $\tilde{\chi}_1^+ \tilde{\chi}_1^-$ and $\tilde{\chi}_1^\pm \tilde{\chi}_1^0$ events. While this is not a large efficiency, it has the advantage of further reducing backgrounds from the very beginning. A photon tag trigger was also considered, but was not found to be competitive with the $\not{E}_T$ trigger.

The main physics background after the trigger, but before any STUB requirements, is $Z(\to \nu\overline{\nu}) + \mathrm{jet}$, which has an effective cross section after our triggering requirements of $\sigma_{\mathrm{eff}} \sim 10^3$ fb. Before STUB requirements, pure QCD backgrounds are two orders of magnitude larger than the $Z(\to \nu\overline{\nu}) + \mathrm{jet}$ background after requiring $\not{E}_T > 35\,\mathrm{GeV}$, i.e., $\sigma_{\mathrm{eff}} \sim 10^5$ fb. The requirement of an isolated, charged track reduces this background by at least a factor 10^{-3} [21]. A further requirement of $\geqslant 2$ MIP energy deposit on all 6 SVX layers contributes another factor of $\sim 10^{-3}$. Therefore, we estimate a background cross section below about 0.1 fb. A cut of $p_T > 30\,\mathrm{GeV}$ on the track may be sufficient without the 2MIP requirement. For a first estimate of sensitivity, we assume that the backgrounds are negligible after requiring one or more STUB tracks.

The cross sections for the SMET and SMET6 (i.e., $\beta < 0.6$ being required for the latter) signals are plotted as a function of $m_{\tilde{\chi}_1^\pm}$ in Figs. 6 and 7 in comparison to the DIT and DIT6 signals. The corresponding three event mass limits are given in Fig. 12, including results for $\Delta m_{\tilde{\chi}_1} = 250$ and 300 MeV. These latter points show that only the SNT and SMET signals will give a background-free cross section for $\Delta m_{\tilde{\chi}_1}$ as large as 300 MeV.

We have also compared the SMET cross section to the cross section obtained by requiring two STUB's without any cut on missing energy (not plotted). One finds that the SMET efficiency is higher than that for two STUB's. Thus, assuming that the SMET signal is background free, it is only if the one STUB, i.e., SNT, signal is also background free that one

would gain by modifying the triggering systems at CDF and DØ so that a STUB could be directly triggered on using the SVX alone.

Finally, Fig. 9 shows the SKMET and SKMET6 cross sections at DØ obtained by adding to the SMET and SMET6 cuts the requirement that the chargino decay prior to 50 cm, so that one could see in the tracker the KINK produced by the chargino decay to a soft pion. For both $\Delta m_{\tilde{\chi}_1} = 140$ and 142.5 MeV, we see very little difference between these two cross sections. Thus, one could look for KINK's with little sacrifice in efficiency.

5. HIP signatures

As $\Delta m_{\tilde{\chi}_1}$ increases above 250 MeV, the chargino, on average, passes through fewer and fewer layers of the SVX. Consequently, it becomes increasingly difficult to reconstruct the SVX track and determine its p_T. In addition, the number of dE/dx samplings decreases and it becomes progressively more difficult to determine whether or not it is heavily ionizing. The STUB signatures become very inefficient. The precise point at which the SMET and SMET6 signals (that can be implemented using current DØ and CDF trigger designs) become untenable must be determined by the experimental groups. One could be hopeful that the reach in $m_{\tilde{\chi}_1^\pm}$ of these signals might be increased for $\Delta m_{\tilde{\chi}_1} < 300$ MeV or so by looking for tracks that penetrate some, but not all, of the SVX layers. Such signals might be relatively clean if one could also see the KINK of the $\tilde{\chi}_1^\pm \to \pi^\pm \tilde{\chi}_1^0$ decay in the SVX. But, it seems very unlikely that one could go much beyond $\Delta m_{\tilde{\chi}_1} = 500$ MeV ($c\tau = 0.1$ cm). Above some point in the $\Delta m_{\tilde{\chi}_1} = 300-500$ MeV range, the only visible sign of the chargino will be the high-impact parameter of the soft charged pion emitted in $\tilde{\chi}_1^\pm$ decay. Aside from needing a means for triggering on HIP tracks, we will see that substantial additional requirements must be imposed to control the backgrounds. As a baseline for this analysis, we use the impact parameter resolution σ_b of the upgraded SVX of the CDF detector, described earlier and detailed in Ref. [11]. As before, we assume that the SVX will have the proposed, extra layer $L00$ at a radius of roughly 1.6 cm. If the chargino decays before this radius, we use the $L00$ parametrization of σ_b. Otherwise, if a decay occurs between 1.6 and 3.0 cm, we use the $L0$ resolution. For a pion track of $p_T = 75$ MeV, this corresponds to σ_b of 0.28 (0.37) mm using $L00$ ($L0$); the corresponding large p_T limits are roughly 0.012 (0.014) mm. We require $b/\sigma_b > 5$ to eliminate fakes, which means the detector is not sensitive to $b < 0.06$ (0.07) mm. Such charged tracks, with b larger than five times the resolution, will be denoted as HIP's.

Unlike the STUB signature, the HIP signature has irreducible backgrounds. The best results are obtained using events that pass our $\gamma + \not{E}_T$ requirements. The HIP backgrounds for the monojet$+\not{E}_T$ event sample are much larger. In any hard scattering process, fragmentation and hadronization of hard jets and beam remnants can produce particles in the central rapidity region with $\gamma c\tau$ on the order of 0.1–10 cm that decay to charged tracks: K_S^0, D, B, Λ, Σ, Ξ, Ω. To reduce this background without substantially reducing the signal, we impose a number of additional cuts:

$$75\ \text{MeV} < p_T^{\text{HIP}} < 1\ \text{GeV}, \quad E_T(\Delta R < 0.4) < 2\ \text{GeV},$$
$$N_{\text{tracks}} = 1. \tag{2.8}$$

The $p_T < 1$ GeV cut is not optimized. It is 100% efficient for the soft charged pions emitted in chargino decays in the models considered here, but strongly suppresses the many backgrounds that tend to yield HIP's with large p_T.

The $p_T > 75$ MeV cut is imposed because σ_b is increasing quickly below this value.

The $E_T(\Delta R < 0.4) < 2$ GeV cut is designed to remove HIP's directly associated with hard jets, which (by definition) have substantial transverse energy in particles nearby a $p_T < 1$ GeV HIP.

Some background is removed by requiring that only one charged track is associated with a given impact parameter (i.e., most $K_S^0 \to \pi^+\pi^-$, $\Lambda^0 \to p^+\pi^-$, etc., decays can be reconstructed and removed when one of the tracks has a large b).

Since heavy flavor is always produced in pairs from the parton sea, it may be possible to tag both hadrons and eliminate part of the background ($ss \to \Sigma^+ K_S^0 + X$), but we have not included this in our analysis. Nor have we used the fact that some of the decays with a single charged track can be explicitly reconstructed [e.g., $\Sigma^+ \to p^+\pi^0(\to \gamma\gamma)$]. After our cuts, of all the long-lived particles noted earlier, only events containing the baryons Σ^+, Σ^-, Ξ, and Ω survive. Additional backgrounds arise from τ decays in the processes $Z/\gamma^*(\to \tau^+\tau^-) + \gamma$ and $W(\to \tau\nu_\tau) + \gamma$, but these are insignificant after the $\gamma + \not{E}_T$ cuts.

After the cuts listed above, PYTHIA predicts that about 14 fb of background remains in the single HIP signal and a fraction of a fb in the double HIP signal, with a tail in the impact parameter distribution extending out to the $L0$ radius. For any $\Delta m_{\tilde{\chi}_1} \gtrsim 200$ MeV, the impact parameter distribution for the signal is quite similar to that for the background. This is illustrated in Fig. 10 for the case of $m_{\tilde{\chi}_1^\pm} = 56$ GeV and $\Delta m_{\tilde{\chi}_1} = 300$ MeV. As a result, no additional cuts on b appear to be useful and the HIP search is reduced to a simple counting experiment. In order to check the PYTHIA computation of the background from baryons with delayed decays that dominate the impact parameter distribution, it will be very useful to measure this same component of the impact parameter distribution in $Z(\to e^+e^-, \mu^+\mu^-) + \gamma$. This will allow considerable control of systematic errors in the background predictions. In the absence of a cross check, the results presented here should be considered only rough estimates.

After requiring $S/B > 0.2$, the integrated luminosity required to either exclude a chargino of a given mass at the 1.96σ (95% C.I.) level or discover it at the 5σ level is plotted in Figs. 11(a) or 11(b), respectively. For $m_{\tilde{\chi}_1^\pm}$ values above those plotted, S/B falls below the $S/B > 0.2$ criterion that we impose. We note that the HIP signal for small $\Delta m_{\tilde{\chi}_1}$ is quite weak. This is because most decays are such that the chargino passes through the SVX before decaying. In this case, one

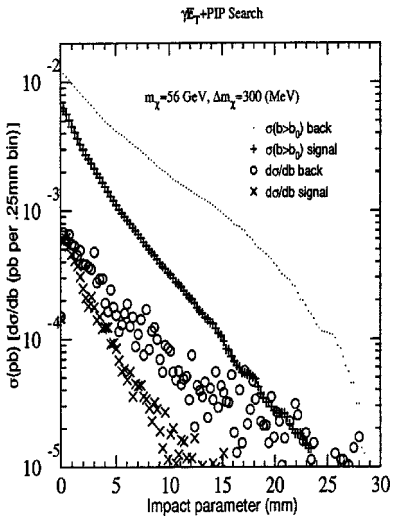

FIG. 10. Impact parameter distributions for the signal and background. We plot the differential cross section, $d\sigma/db$ (in units of pb/0.25 mm), and the integrated cross section, $\int_b^\infty (d\sigma/db')db'$ (in pb units). The signal shown here is for $m_{\tilde{\chi}_1^\pm}=56$ GeV and $\Delta m_{\tilde{\chi}_1}=300$ MeV. The fluctuations in the distributions are from the statistics of the Monte Carlo simulation.

should look for the STUB and STUB+KINK signatures discussed earlier, for which backgrounds are negligible and much better sensitivity is possible. Clearly, the STUB and HIP signals are complementary with viability for the latter rising with increasing $\Delta m_{\tilde{\chi}_1}$ as mass reach for the former declines. As $\Delta m_{\tilde{\chi}_1}$ increases, the HIP+γ+$\not{E}_T$ signal increases in viability until $\Delta m_{\tilde{\chi}_1} \lesssim 300$ MeV. By $\Delta m_{\tilde{\chi}_1}=600$ MeV, the typical impact parameter for the decay pion declines below 100 μm, and cannot be resolved by the SVX; the HIP signal can only probe $m_{\tilde{\chi}_1^\pm}$ values below the roughly 70 GeV limit set by the DELPHI analysis for $\Delta m_{\tilde{\chi}_1} \geqslant 600$ MeV (assuming a heavy sneutrino).

Some further discussion of the difference between the

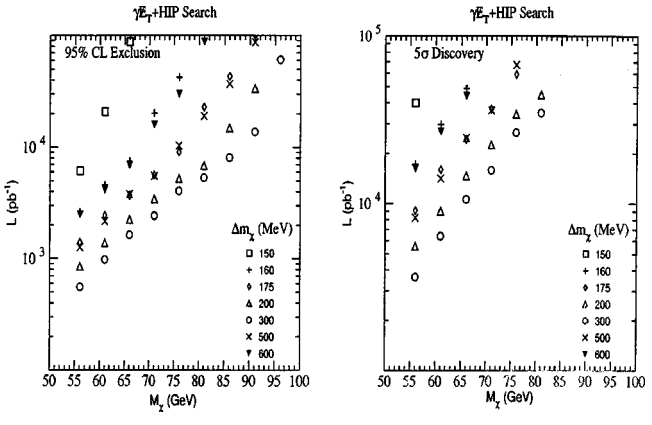

FIG. 11. Reach for the $\gamma+\not{E}_T$ searches after requiring one or more HIP for different mass splittings $\Delta m_{\tilde{\chi}_1}$. The left curve shows the 95% C.L. exclusion; the right shows the 5σ discovery. We require $S/B>0.2$ and at least 3 (5) expected events for exclusion (discovery).

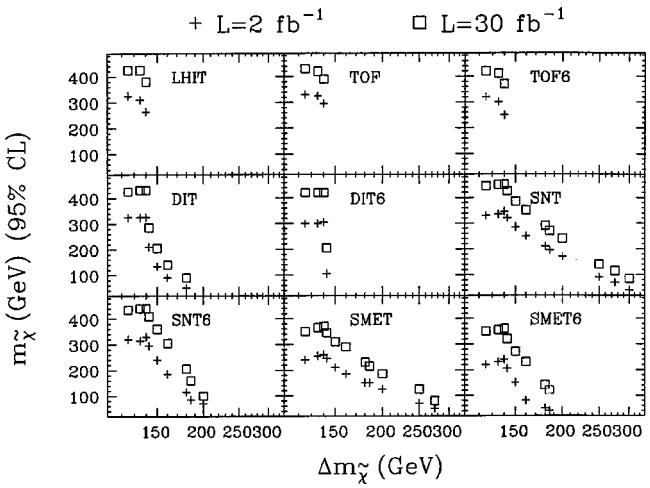

FIG. 12. 95% C.L. lower limits on $m_{\tilde{\chi}_1^\pm}$ as a function of $\Delta m_{\tilde{\chi}1}$ for ''background-free'' signatures at Run II with $L=2$ fb^{-1} and $L=30$ fb^{-1}.

STUB and HIP signals is perhaps useful. First, it is the large background that restricts the mass reach of the HIP signal, whereas the biggest limitation on the STUB signals is associated with the chargino lifetime. Second, the STUB signals are background free, while the HIP signal is not. The key to eliminating backgrounds to STUB signatures is that the $\Sigma^\pm, \ldots$ hadrons that can give an SVX track will decay to particles that pass all the way through the CT and give sizeable hadronic calorimeter energy deposits; in addition, one or more of the decay products are normally (i.e., except for distribution tails where the charged decay products all have small p_T) visible as a full CT track. If there is some remaining background, then one would have to also look to see if the STUB is heavily ionizing. The $\Sigma^\pm, \ldots$ background tracks would all be minimal ionizing, so that a $\beta<0.6$ requirement would certainly eliminate the remaining background. The crossover point between the signals depends on whether the heavy-ionization requirement is necessary to remove the background. For $\Delta m_{\tilde{\chi}_1}=180$ MeV, Fig. 12 shows that with $L=30$ fb^{-1}, the SMET (SMET6) signals (which include the $\not{E}_T>35$ GeV trigger requirement) can be used to exclude at 95% C.I. any $m_{\tilde{\chi}_1^\pm} \lesssim 240$ GeV ($\lesssim$140 GeV). In contrast, for $\Delta m_{\tilde{\chi}_1}=180$ MeV the HIP signal can only probe $m_{\tilde{\chi}_1^\pm} \lesssim 80$ GeV. For $\Delta m_{\tilde{\chi}_1}=200$ MeV, the SMET signal still probes up to $m_{\tilde{\chi}_1^\pm} \lesssim 190$ GeV, but the SMET6 signal falls just below the 95% C.L. For $\Delta m_{\tilde{\chi}_1}=300$ MeV, the SMET and HIP signals both probe up to $m_{\tilde{\chi}_1^\pm} \lesssim 90$ GeV.

Various exotic signals can be envisioned that might probe $\Delta m_{\tilde{\chi}_1}$ values above 600 MeV, but we only comment on them here. For example, if $\Delta m_{\tilde{\chi}_1} > m_s + m_c$ the decay $\tilde{\chi}_1^\pm \to D_s^* \tilde{\chi}_1^0$ may occur, leading to a D_s meson that carries most of the D_s^*'s momentum. When combined with an $\not{E}_T$ trigger, the signature would be quite distinctive since the D_s will not be associated with a jet. However, the event rate for such an ''exclusive'' channel might be small.

III. SUMMARY OF RESULTS, DISCUSSION, AND CONCLUSION

In the previous sections, we considered several signatures for chargino production in models with near mass degeneracy between the lightest chargino and neutralino. The motivation for these models is described in the Introduction. A brief summary of the signatures appears in Table III. We have seen that there is a natural boundary near a mass splitting of $\Delta m_{\tilde{\chi}_1} \sim 300\,\mathrm{MeV}$.

For values of $\Delta m_{\tilde{\chi}_1} \lesssim 300\,\mathrm{MeV}$ (mass region *A*), signals are based on observing a long-lived chargino as a semistable, isolated track in the detector. The most unique signals are the long, heavily ionizing track (LHIT) signal and the delayed time-of-flight (TOF) signal. These are present for events in which the chargino does not decay before reaching the muon chambers. For events in which the chargino decays before the muon chambers, but still produces a track of substantial length, the relevant signals are the disappearing-isolated-track (DIT) signal and the short-isolated-SVX-track (STUB) signal. The LHIT and TOF signals are dominant if $\Delta m_{\tilde{\chi}_1}$ is very small (implying a very long chargino lifetime), but the latter signals quickly turn on as $\Delta m_{\tilde{\chi}_1}$ is increased, becoming the primary signals as $\Delta m_{\tilde{\chi}_1}$ is increased to values above m_π.

All these signals are distinct enough to be possibly background free. Because of the subtle nature of these signals, in estimating the the range of $m_{\tilde{\chi}_1^\pm}$ values to which they can be sensitive for any given $\Delta m_{\tilde{\chi}_1}$, we have imposed cuts and/or requirements such that the backgrounds should be negligible, even at the expense of some signal rate.

For $\Delta m_{\tilde{\chi}_1} \gtrsim 300\,\mathrm{MeV}$, the chargino has an average lifetime such that the background free signals have too low an event rate (at the Tevatron) and we are forced to consider signals with substantial backgrounds from physics and mismeasurement sources. There are two primary signals in this latter category, but the most sensitive one can only be used for $300\,\mathrm{MeV} \lesssim \Delta m_{\tilde{\chi}_1} \lesssim 600\,\mathrm{MeV}$ (mass region *B*). It relies on observation of a high-impact-parameter (HIP) pion from the chargino decay in association with a photon tag-trigger and large $\not{E}_T$. For $600\,\mathrm{MeV} \lesssim 10-20\,\mathrm{GeV}$ (mass region *C*), the chargino decay is essentially prompt, and we are forced to use the very insensitive signal of a photon tag-trigger plus large $\not{E}_T$ to search for chargino production.

The importance of particular detector components and triggers for such signatures, as outlined in the main body of this paper, should be carefully reviewed by the CDF and DØ Collaborations. The silicon tracker (SVX), central tracking system (CT), preshower (PS), electromagnetic and hadronic calorimeters (EC and HC), time-of-flight (TOF) measurement and muon chambers (MC's) all play crucial roles that change as a function of $\Delta m_{\tilde{\chi}_1}$. (Our detector notation is summarized in Table II.)

We will now summarize the Tevatron mass reach in $m_{\tilde{\chi}_1^\pm}$ that can be achieved in the $M_2 < M_1 \ll |\mu|$ scenario (1), assuming that the gluino, squarks and sleptons are all too heavy to have significant production rate (as is entirely possible).

Region (A). For $\Delta m_{\tilde{\chi}_1}$ values $\lesssim$200–300 MeV, one considers the background-free signals summarized above, which will have the most substantial mass reach in $m_{\tilde{\chi}_1^\pm}$. The $L = 2\,\mathrm{fb}^{-1}$ and $L = 30\,\mathrm{fb}^{-1}$ 95% C.L. (3 events, no background) limits on $m_{\tilde{\chi}_1^\pm}$ deriving from these signals are summarized in Fig. 12. We give a brief verbal summary.

$\Delta m_{\tilde{\chi}_1} < m_\pi$: For such $\Delta m_{\tilde{\chi}_1}$, the average $c\tau$ of the chargino is of order a meter or more. The LHIT and TOF signals are prominent, but the DIT and STUB signals appear if $\Delta m_{\tilde{\chi}_1}$ is not extremely small. These arise as a result of the exponential form of the $c\tau$ distribution in the chargino rest frame, which implies that the chargino will decay over a range of radii within the detector. One must also include the event-by-event variation of the boosts imparted to the chargino(s) during production.

The LHIT signature can probe masses in the range 260–325 (380–425) GeV for $L = 2\,\mathrm{fb}^{-1}$ ($30\,\mathrm{fb}^{-1}$), the lower reach applying for $\Delta m_{\tilde{\chi}_1} \sim m_\pi$ and the highest reach applying for any $\Delta m_{\tilde{\chi}_1} \lesssim 125\,\mathrm{MeV}$. The reach of the TOF signature is nearly identical to that of the LHIT signature.[5]

The DIT signature has a reach[6] of 320 (425) GeV for $120\,\mathrm{MeV} \lesssim \Delta m_{\tilde{\chi}_1} \lesssim m_\pi$, and, in particular, is more efficient than the LHIT and TOF signals for $\Delta m_{\tilde{\chi}_1} \sim m_\pi$. The DIT signature reach drops by about 20 GeV with a $\beta < 0.6$ cut (DIT6) designed to require that the chargino track be heavily ionizing.

The STUB signature with no additional trigger (SNT) can reach to $\simeq$340 (450) GeV for $120\,\mathrm{MeV} \lesssim \Delta m_{\tilde{\chi}_1} \lesssim m_\pi$, where the mass reach drops by 10–20 GeV if $\beta < 0.6$ is required. However, neither DØ nor CDF can use STUB information at level 1 in their current design.

With the addition of a standard $\not{E}_T$ trigger, the resulting STUB signature (SMET) will be viable with the present detectors, reaching to 240–260 (350–375) GeV for $120\,\mathrm{MeV} \lesssim \Delta m_{\tilde{\chi}_1} \lesssim m_\pi$, which numbers drop by about 10 GeV if $\beta < 0.6$ is required (SMET6).

$m_\pi \lesssim \Delta m_{\tilde{\chi}_1} \lesssim 200-300\,\mathrm{MeV}$: The LHIT and TOF signatures disappear, since almost all produced charginos decay before reaching the MC or TOF.

The DIT signature remains as long as the $\beta < 0.6$ (heavily

[5]The primary difference between the LHIT and TOF signals is that the LHIT signal requires $\beta\gamma < 0.85$ for heavy ionization, whereas the effective cutoff on $\beta\gamma$ imposed by the TOF delay requirement allows much larger $\beta\gamma$ to also contribute. That the maximum reach of the two signals is essentially the same is somewhat accidental. It happens that the chargino production cross sections are large enough that charginos with rather large mass can be probed and such massive charginos are produced with low β. Thus, a cut requiring low β is highly efficient. This is illustrated, for example, by comparing the TOF to the TOF6 results in Fig. 12. This same accident is generic to all the signals discussed, so long as $\Delta m_{\tilde{\chi}_1} < m_\pi$.

[6]We did not study lower $\Delta m_{\tilde{\chi}_1}$ values since they are highly improbable after including radiative correction contributions to $\Delta m_{\tilde{\chi}_1}$.

TABLE IV. Summary of the best signals at Run II for $\tilde{\chi}_1^+\tilde{\chi}_1^-$ and $\tilde{\chi}_1^\pm\tilde{\chi}_1^0$ production and important detector components and measurements as a functon of $\Delta m_{\tilde{\chi}_1}$. Mass reaches quoted are 95% C.L. for $L=30\,\mathrm{fb}^{-1}$. Detector component notation is summarized in Table II. Signal definitions are summarized in Table III. The PS, EC, or HC veto requires no preshower, small EC, or small HC energy deposits in a $\Delta R<0.4$ cone around the $\tilde{\chi}_1^\pm$ track candidate. $p_T(p_T^\pi)$ is the p_T of the $\tilde{\chi}_1^\pm$ ($\pi^\pm$ from $\tilde{\chi}_1^\pm\to\pi^\pm\tilde{\chi}_1^0$). b^π is the $\pi^\pm$ impact parameter.

$\Delta m_{\tilde{\chi}_1}$ (MeV)	$c\tau$ (cm)	Best Run II signature(s)	Tigger	Crucial measurements and associated detector components	Reach (GeV)
0	∞	TOF	MC	TOF, p_T(SVX+CT)	460
		LHIT	MC	p_T(SVX+CT), dE/dx (SVX+CT+PS)	450
125	1155	TOF	MC	TOF, p_T(SVX+CT)	430
		LHIT	MC	p_T(SVX+CT), dE/dx (SVX+CT+PS)	425
		DIT	CT	p_T(SVX+CT), HC veto	425
		DIT6	CT	same+dE/dx (SVX+CT+PS),	420
135	754	LHIT	MC	p_T(SVX+CT), dE/dx (SVX+CT+PS),	425
		TOF	MC	TOF, p_T(SVX+CT)	420
		DIT	CT	p_T(SVX+CT), HC veto	430
		DIT6	CT	same+dE/dx (SVX+CT+PS)	420
140	317	DIT	CT	p_T(SVX+CT), HC veto	430
		DIT6	CT	same+dE/dx (SVX+CT+PS)	420
142.5	24	SMET	$\not{E}_T$	p_T(SVX), PS+EC+HC veto	345
		SMET6	$\not{E}_T$	same+dE/dx (SVX)	320
150	11	SMET	$\not{E}_T$	p_T(SVX), PS+EC+HC veto	310
		SMET6	$\not{E}_T$	same+dE/dx (SVX)	270
185	3.3	SMET	$\not{E}_T$	p_T(SVX), PS+EC+HC veto	215
		SMET6	$\not{E}_T$	same+dE/dx (SVX)	120
200	2.4	SMET	$\not{E}_T$	p_T(SVX), PS+EC+HC veto	185
250	1.0	SMET	$\not{E}_T$	p_T(SVX), PS+EC+HC veto	125
300	0.56	HIP	$\gamma,\not{E}_T$	b^π(SVX,$L0$), $p_T^\gamma,\not{E}_T,p_T^\pi$(CT), EC+HC veto	95
600	0.055	HIP	$\gamma,\not{E}_T$	b^π(SVX,$L00$), $p_T^\gamma,\not{E}_T,p_T^\pi$(CT), EC+HC veto	75
750-?	$\sim$0	$\gamma+\not{E}_T$	$\gamma,\not{E}_T$	$p_T^\gamma,\not{E}_T$	$<$60

ionizing) requirement is not necessary to eliminate backgrounds. If we require $\beta<0.6$, there is a mismatch with the requirement that the chargino pass through the CT—once $\Delta m_{\tilde{\chi}1}$ is above 145 MeV, and the entire signal is generated by large boosts in the production process which is in conflict with requiring small β.

The SNT signature probes $m_{\tilde{\chi}_1^\pm}\lesssim 300\,\mathrm{GeV}$ ($\lesssim$400 GeV) for $\Delta m_{\tilde{\chi}1}\sim m_\pi$ and $L=2\,\mathrm{fb}^{-1}$ ($L=30\,\mathrm{fb}^{-1}$). For $\Delta m_{\tilde{\chi}1}$ as large as 300 MeV, it alone among the background-free channels remains viable, probing $m_{\tilde{\chi}_1^\pm}\lesssim 70\,\mathrm{GeV}$ ($\lesssim$95 GeV). Certainly, it would extend the DELPHI limits at LEP2 even in the heavy sneutrino case. We recall that these were $\sim$90 GeV for $\Delta m_{\tilde{\chi}1}<200\,\mathrm{MeV}$ and $\sim$70 GeV for $200\,\mathrm{MeV}\leqslant\Delta m_{\tilde{\chi}1}\leqslant 3\,\mathrm{GeV}$. But, as stated above, the SNT signature will not be possible without a level-1 SVX trigger.

The STUB+$\not{E}_T$, SMET, and SMET6 signatures are fully implementable at Run II and have a reach that is only about 20 GeV lower than their SNT and SNT6 counterparts. Unfortunately, this would not extend the DELPHI limits unless the sneutrino is light.

Region (B). For $300\,\mathrm{MeV}\lesssim\Delta m_{\tilde{\chi}1}\lesssim 600\,\mathrm{MeV}$, the high-impact-parameter (HIP) signal (a $\gamma+\not{E}_T$ tag for events yields the smallest backgrounds) is very useful despite the large background from production of $\Sigma^\pm$,… hadrons. It would yield a 95% C.L. lower bound of 95 GeV (75 GeV) on $m_{\tilde{\chi}_1^\pm}$ for $\Delta m_{\tilde{\chi}1}=300\,\mathrm{MeV}$ ($\Delta m_{\tilde{\chi}1}=600\,\mathrm{MeV}$) for $L=30\,\mathrm{fb}^{-1}$. This is to be compared to the $\sim$70–75 GeV lower bound obtained in the current DELPHI analysis of their LEP2 data for this same range of $\Delta m_{\tilde{\chi}1}$ if the sneutrino is heavy. (If the $\tilde{\nu}$ is light, then there is no useful LEP2 limit if $60\,\mathrm{MeV}\leqslant\Delta m_{\tilde{\chi}1}\leqslant 500\,\mathrm{MeV}$, but LEP data requires $m_{\tilde{\chi}_1^\pm}>45\,\mathrm{GeV}$.) With only $L=2\,\mathrm{fb}^{-1}$ of data, the HIP analysis would only exclude $m_{\tilde{\chi}_1^\pm}<68\,\mathrm{GeV}$ ($<53\,\mathrm{GeV}$) for $\Delta m_{\tilde{\chi}1}=300\,\mathrm{MeV}$ ($\Delta m_{\tilde{\chi}1}=600\,\mathrm{MeV}$).

Region (C). For $\Delta m_{\tilde{\chi}1}\gtrsim 600\,\mathrm{MeV}$, up to some fairly large value (we estimate at least 10–20 GeV), the chargino decay products are effectively invisible at a hadron collider and the most useful signal is $\gamma+\not{E}_T$. However, this signal at best probes $m_{\tilde{\chi}_1^\pm}\lesssim 60\,\mathrm{GeV}$ (for any $L>2\,\mathrm{fb}^{-1}$), whereas the DELPHI analysis of their LEP2 data already excludes $m_{\tilde{\chi}_1^\pm}\leqslant 70\,\mathrm{GeV}$ for $500\,\mathrm{MeV}\leqslant\Delta m_{\tilde{\chi}1}\leqslant 3\,\mathrm{GeV}$ (if the sneutrino is heavy—only $\leqslant$50–52 GeV if the sneutrino is light) and $m_{\tilde{\chi}_1^\pm}\leqslant 90\,\mathrm{GeV}$ for $\Delta m_{\tilde{\chi}1}>3\,\mathrm{GeV}$.

An overall summary of the signals and their mass reach at the Tevatron for detecting $\tilde{\chi}_1^+\tilde{\chi}_1^-$ and $\tilde{\chi}_1^\pm\tilde{\chi}_1^0$ production in the $M_2<M_1\ll|\mu|$ scenario (1) appears in Table IV.

All the above mass limits assume that the gluino is quite heavy and rarely produced at the Tevatron. If it is not too much heavier than the chargino, then all the above signals will have additional event rate coming from $\tilde{g}\tilde{g}$ pair production followed by $\tilde{g}\to\tilde{\chi}_1^\pm q'\bar{q}$ decays. The effect of $\tilde{g}\tilde{g}$ pair production on the LHIT, TOF, DIT, SNT, SMET, and HIP signatures depends strongly on the mass splitting between the gluino and the chargino as well as on $\Delta m_{\tilde{\chi}1}$, so we did not explicitly consider possible enhancements to these signatures here. Instead, we focused on the fact that gluino production will provide a critical increase in the mass reach when neither the chargino track nor its decay products are visible, and the only signatures are those dependent primarily upon missing transverse energy. This is the case if $\Delta m_{\tilde{\chi}1}$ is above 600 MeV but below the point at which the chargino decay products can be seen as energetic jets or leptons. For example, we explicitly considered the extreme of $m_{\tilde{g}}\sim m_{\tilde{\chi}_1^\pm}$ (which is quite natural in some string models—see Introduction). In this case, we found that a monojet$+\not{E}_T$ signal will probe (at 95% C.L.) $m_{\tilde{g}}\sim m_{\tilde{\chi}_1^\pm}<150\,\mathrm{GeV}$, while the $\gamma+\not{E}_T$ signal will probe $m_{\tilde{g}}\sim m_{\tilde{\chi}_1^\pm}<175\,\mathrm{GeV}$. (Both numbers assume that $S/B>0.2$ is required for a viable signal in the presence of large background.)

In some of the models in question, it is entirely possible that $\Delta m_{\tilde{\chi}1}$ is quite substantial (>20 GeV), and the signals considered in this paper are not very useful. If the gluino is heavy, then one should explore the potential of the trilepton signal coming from $\tilde{\chi}_1^\pm\tilde{\chi}_2^0$ production. However, this is a suppressed cross section when both the lightest neutralino and lightest chargino are W-ino like. Standard MSUGRA studies do not apply without modification; the cross section must be rescaled and the lepton acceptance recalculated as a function of $\Delta m_{\tilde{\chi}1}$. If the gluino is close in mass to the chargino, then the standard multijet$+\not{E}_T$ signal will be viable when $\Delta m_{\tilde{\chi}1}$ is large enough for the jets in $\tilde{\chi}_1^\pm\to q'\bar{q}\tilde{\chi}_1^0$ decay to be visible. The like-sign dilepton signal will also emerge for large $\Delta m_{\tilde{\chi}1}$, as the leptons in $\tilde{\chi}_1^\pm\to l\nu\tilde{\chi}_1^0$ become energetic. Since both signals will have substantial backgrounds, a detailed study is required to determine their exact mass reach as a function of $\Delta m_{\tilde{\chi}1}$. If the gluino has a moderate mass but $m_{\tilde{g}}-m_{\tilde{\chi}_1^\pm}$ is large enough, then the extra jets from $\tilde{g}\to q'\bar{q}\tilde{\chi}_1^\pm$ become visible and nearly all events contain more than one jet. The multijet$+\not{E}_T$ signal becomes viable as shown in Ref. [4]. (We note that the reach of the monojet $+\not{E}_T$ signature explored here deteriorates once the multijet $+\not{E}_T$ signal becomes substantial. For instance, we find that the former signal is no longer useful once $m_{\tilde{g}}-m_{\tilde{\chi}_1^\pm}>10\,\mathrm{GeV}$.) Of course, additional SUSY signals will emerge if some of the squarks, sleptons and/or sneutrinos are light enough (but still heavier than the $\tilde{\chi}_1^\pm$) that their production rates are substantial. In particular, leptonic signals from the decays [e.g., $\tilde{l}_L^\pm\to l^\pm\tilde{\chi}_1^0$ or $\tilde{\nu}_l\to l^\pm\tilde{\chi}_1^\mp$ in scenario (1)] would be present.

If one or more of the signatures outlined here are observed, then the precise values of $m_{\tilde{\chi}_1^\pm}$ and $\Delta m_{\tilde{\chi}1}$ will be of significant theoretical interest. $m_{\tilde{\chi}_1^\pm}$ will be determined on an event-by-event basis if the chargino's momentum and velocity can both be measured. For the LHIT signal, p will be measured by the curvature of the track in the SVX and in the CT. The velocity will be measured by the ionization energy deposit in the SVX, CT, and PS. In the case of the TOF signal, there will be, in addition, an independent time-of-flight determination of β. For the DIT signal, the SVX+CT curvatures give a measurement of p and the SVX+CT+PS ionization energy deposits provide a determination of β. For the SNT and SMET signals, p and β are measured by curvature and ionization (respectively) in the SVX. (Note that, in all these cases, accepting only events roughly consistent with a given value of $m_{\tilde{\chi}_1^\pm}$ will provide further discrimination against backgrounds.) However, for the HIP and $\gamma+\not{E}_T$ signals $m_{\tilde{\chi}_1^\pm}$ can only be estimated from the absolute event rate. As regards $\Delta m_{\tilde{\chi}1}$, it will be strongly constrained by knowing which signals are present and their relative rates. In addition, if the soft charged pion can be detected, its momentum distribution, in particular the endpoint thereof, would provide an almost direct determination of $\Delta m_{\tilde{\chi}1}$.

Given the possibly limited reach of the Tevatron when the lightest neutralino and chargino are nearly degenerate, it will be very important to extend these studies to the LHC. A particularly important issue is the extent to which the large $c\tau$ tails of the $\tilde{\chi}_1^\pm$ decay distributions can yield a significant rate in the background-free channels studied here. Hopefully, as a result of the very high event rates and boosted kinematics expected at the LHC, the background-free channels will remain viable for significantly larger $\Delta m_{\tilde{\chi}1}$ and $m_{\tilde{\chi}_1^\pm}$ values than those to which one has sensitivity at the Tevatron. In this regard, a particularly important issue for maximizing the mass reach of these channels will be the extent to which tracks in the silicon vertex detector and/or in the central tracker can be used for triggering in a high-luminosity environment.

While finalizing the details of this study, two other papers [22,23] appeared on the same topic. Some of the signatures discussed here are also considered in those papers. Our studies are performed at the particle level and contain the most important experimental details.

ACKNOWLEDGMENTS

This work was supported by the Department of Energy and by the Davis Institute for High Energy Physics. We benefited greatly from conversations with H. Frisch, G. Grim, R. Lander, G. Landsberg, D. Stuart, R. Van Kooten, and J. Womersley.

[1] H. Baer, K. Cheung, and J. Gunion, in Proceedings of the Tevatron SUSY/Higgs RunII Workshop, edited by M. Carena and J. Lykken.
[2] A. Brignole, L. E. Ibanez, and C. Munoz, Nucl. Phys. **B422**, 125 (1994); **B436**, 747(E) (1995); hep-ph/9707209.
[3] C. H. Chen, M. Drees, and J. F. Gunion, Phys. Rev. Lett. **76**, 2002 (1996).
[4] C. H. Chen, M. Drees, and J. F. Gunion, Phys. Rev. D **55**, 330 (1997).
[5] C. H. Chen, M. Drees, and J. F. Gunion, Phys. Rev. Lett. **82**, 3192(E) (1999).
[6] G. F. Giudice, M. A. Luty, H. Murayama, and R. Rattazzi, J. High Energy Phys. **12**, 027 (1998).
[7] L. Randall and R. Sundrum, Nucl. Phys. **B557**, 79 (1999).
[8] G. Anderson, C. H. Chen, J. F. Gunion, J. Lykken, T. Moroi, and Y. Yamada, in *New Directions for High Energy Physics*, Proceedings of the Snowmass96 Summer Study, 1996, Snowmass, CO, edited by D. G. Cassel, L. T. Gennari, and R. H. Siemann, p. 669, hep-ph/9609457.
[9] S. Mizuta, D. Ng, and M. Yamaguchi, Phys. Lett. B **300**, 96 (1993); A. Papadopoulos and D. Pierce, Nucl. Phys. **B430**, 278 (1994); D. Pierce, J. Bagger, K. Matchev, and R.-J. Zhang, *ibid.* **B491**, 3 (1997).
[10] S. Thomas and J. D. Wells, Phys. Rev. Lett. **81**, 34 (1998).
[11] CDF II Collaboration, R. Blair *et al.*, proposal for Enhancement of the CDF II Detector: An Inner Silicon Layer and A Time of Flight Detector, Fermilab-Proposal-909.
[12] DØ Collaboration, G. Landsberg (private communication); D. Cutts and G. Landsberg, hep-ph/9904396.
[13] CDF Collaboration, D. Stuart (private communication).
[14] DELPHI Collaboration, P. Abreu *et al.* CERN-EP/99-37. For the most recent update, see DELPHI Collaboration, S. Paiano, A. Perrotta, T. Rovelli, R. Alemany, and G. Garcia, in HEP'99 Conference, Tampere, Finland, DELPHI 99-84 CONF-271.
[15] T. Sjostrand, Comput. Phys. Commun. **82**, 74 (1994); S. Mrenna, *ibid.* **101**, 232 (1997).
[16] DØ Collaboration, S. Abachi *et al.*, Phys. Rev. Lett. **78**, 3640 (1997).
[17] Run II estimates of the capabilities of the CDF and DØ detectors have been provided in private communications with H. Frisch, G. Grim, R. Lander, G. Landsberg, D. Stuart, R. Van Kooten, and J. Womersley.
[18] F. E. Paige, S. D. Protopescu, H. Baer, and X. Tata, hep-ph/9810440.
[19] K. T. Matchev and D. M. Pierce, Phys. Rev. D **60**, 075004 (1999).
[20] H. Baer, K. Cheung, and J. F. Gunion, Phys. Rev. D **59**, 075002 (1999).
[21] From the transparencies of the talk by Rick Field at the CDF QCD subgroup Meeting, 1999, available at http://www.phys.ufl.edu/~rfield/cdf/rdf_cdf.html.
[22] J. L. Feng, T. Moroi, L. Randall, M. Strassler, and S. Su, Phys. Rev. Lett. **83**, 1371 (1999).
[23] T. Gherghetta, G. F. Giudice, and J. D. Wells, Nucl. Phys. **B559**, 27 (1999).